NASA TECHNICAL NOTE

NASA TN D-6870

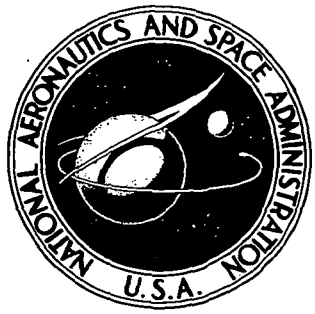

NASA TN D-6870

RING-BAFFLE PRESSURE DISTRIBUTION AND SLOSH DAMPING IN LARGE CYLINDRICAL TANKS

by Harland F. Scholl, David G. Stephens, and Phillip K. Davis

Langley Research Center
Hampton, Va. 23365

NATIONAL AERONAUTICS AND SPACE ADMINISTRATION • WASHINGTON, D. C. • DECEMBER 1972

1. Report No.	2. Government Accession No.	3. Recipient's Catalog No.
NASA TN D-6870		

4. Title and Subtitle	5. Report Date
RING-BAFFLE PRESSURE DISTRIBUTION AND SLOSH DAMPING IN LARGE CYLINDRICAL TANKS	December 1972
	6. Performing Organization Code
7. Author(s)	8. Performing Organization Report No.
Harland F. Scholl, David G. Stephens, and Phillip K. Davis	L-8352
	10. Work Unit No.
9. Performing Organization Name and Address	975-72-51-06
NASA Langley Research Center Hampton, Va. 23365	11. Contract or Grant No.
	13. Type of Report and Period Covered
12. Sponsoring Agency Name and Address	Technical Note
National Aeronautics and Space Administration Washington, D.C. 20546	14. Sponsoring Agency Code

15. Supplementary Notes

16. Abstract

An investigation was conducted to determine the pressure loads and damping associated with rigid ring baffles in relatively large cylindrical tanks. The radial and circumferential pressure distribution, as well as the damping, was measured on a ring baffle subjected to fundamental antisymmetric slosh in a 284-cm-diameter rigid tank. Experimental and analytical data are presented as a function of slosh velocity or amplitude, baffle spacing, and baffle locations both above and below the liquid surface. Results suggest that pressure distributions and damping values can be determined from available theories for the design of single and multiple baffle configurations.

17. Key Words (Suggested by Author(s))	18. Distribution Statement
Slosh damping Baffles Baffle pressures	Unclassified – Unlimited

19. Security Classif. (of this report)	20. Security Classif. (of this page)	21. No. of Pages	22. Price*
Unclassified	Unclassified	42	$3.00

*For sale by the National Technical Information Service, Springfield, Virginia 22151

RING-BAFFLE PRESSURE DISTRIBUTION AND SLOSH DAMPING IN LARGE CYLINDRICAL TANKS

By Harland F. Scholl, David G. Stephens,
and Phillip K. Davis
Langley Research Center

SUMMARY

An investigation was conducted to determine the pressure loads and damping associated with rigid ring baffles in relatively large cylindrical tanks. The radial and circumferential pressure distribution, as well as the damping, was measured on a ring baffle subjected to fundamental antisymmetric slosh in a 284-cm-diameter rigid tank. Experimental and analytical data are presented as a function of slosh velocity or amplitude, baffle spacing, and baffle locations both above and below the liquid surface. Results suggest that pressure distributions and damping values can be determined from available theories for the design of single and multiple baffle configurations.

INTRODUCTION

Antislosh baffles are usually required in liquid-propellant space vehicles to minimize propellant oscillations. The most common configuration consists of rigid rings fitted around the internal periphery of the tank. Such baffles often comprise a high percentage of the tank weight. Therefore, it is important that the baffle design be efficient in terms of the damping per unit of baffle weight. Efficient design of both rigid and flexible baffles requires a detailed understanding of the hydrodynamic loads as well as the damping associated with the baffle configuration.

Numerous studies have been conducted to investigate and develop antislosh devices. Most of these studies have concentrated on the damping provided by various baffle configurations, with much less attention directed toward baffle loads. For example, damping associated with rigid and flexible flat ring baffles mounted in cylindrical tanks is discussed in references 1 to 4, where it is shown that the damping provided by a single ring baffle can be predicted with reasonable accuracy by using semiempirical relationships such as the one presented by Miles in reference 5. The damping provided by a series of ring baffles, as calculated by Helmut F. Bauer, using linear superposition, is shown in reference 1. As noted in reference 2, however, the superposition is inaccurate for closely

spaced baffles. Furthermore, there is no experimental verification for the damping provided by a series of baffles.

Semiempirical theories are presented in reference 6 for the maximum pressure on submerged baffles subjected to oscillatory slosh, as well as for baffles which are uncovered during the slosh cycle and subjected to a slapping or impact action. However, these expressions have not been verified by experiment. An irrotational flow model for the forces and pressures on a single ring baffle, developed by Frank C. Liu, is compared with experimental data in reference 7. Davis, in the appendix of the present paper, develops an expression for pressure which is based on irrotational flow results, similar to that of Liu, and adds a velocity-squared drag term utilizing the measured drag coefficients presented by Keulegan and Carpenter in reference 8. In addition to oscillatory acceleration and velocity terms, the expression accounts for radial and circumferential pressure distributions.

The loads experienced by a ring baffle while submerged and partially submerged in a relatively large tank of oscillatory liquid are examined in this study and compared with available theories. The effects of baffle spacing on pressure loads are included. Damping data for single and multiple baffles are presented to indicate the effectiveness of multiple baffle systems.

SYMBOLS

C coefficient

D plate width or cylinder diameter (as used by Keulegan and Carpenter in ref. 8), cm

d distance from quiescent surface to uppermost baffle, positive when baffle is below quiescent surface, cm

F force, N/cm

g acceleration due to gravity, cm/sec^2

h liquid depth, cm

i imaginary number

K nondimensional parameter, $P/\rho U_{max}^2$ (determined by Keulegan and Carpenter in ref. 8)

N	number of cycles
P	dynamic pressure, N/m^2
ΔR	remainder function
r	tank radius, cm
s	distance between baffles, cm
T	natural period of liquid oscillation, sec
t	time, sec
U	velocity of liquid at baffle location, cm/sec
W	width of baffle, cm
w	complex velocity potential, cm^2/sec
x	coordinate normal to y-coordinate, cm
y	coordinate in direction of plate or baffle width
z	complex variable, cm
β	angle in plane of quiescent surface, measured from antinode position, deg
δ	logarithmic decrement, $\frac{1}{N} \log_e \frac{\zeta_n}{\zeta_{N+n}}$
ζ	displacement amplitude of liquid surface, cm

$\theta = \frac{2\pi t}{T}(57.3)$, deg

θ_{max}	value of θ when $F = F_{max}$, deg
ν	kinematic viscosity, cm^2/sec

ρ liquid mass density, kg/cm^3

$\Phi = 180^o - \theta_{max}$, deg

φ velocity potential, cm^2/sec

ψ stream function, cm^2/sec

Ω body force potential function, cm^2/sec^2

ω natural circular frequency, rad/sec

Subscripts:

d drag

I inertia

max maximum

n nth cycle of vibration

APPARATUS AND TEST PROCEDURE

Tank

A vertical cylindrical steel tank with a circular cross section and an ellipsoidal bottom was used in the investigation (fig. 1). The tank had an inside diameter of 284 cm and a wall thickness of 1.58 cm. Two relatively long, narrow antiswirl plates were mounted vertically along the tank wall at the desired antinode locations of the fundamental mode to minimize rotational drift of the slosh plane. The pertinent dimensions of the tank are given in figure 2. The tank was considered to be rigid and it remained stationary during the tests.

Baffles

Two ring baffles, each split into two 180^o segments with the separations at the nodal locations of the fundamental antisymmetric slosh mode, were used for these tests. The baffles, which were constructed of 0.32-cm-thick aluminum plate, were 14.2 cm wide and extended to the tank wall, where they were rigidly supported by angle brackets. The distance d from the quiescent surface to the top baffle (fig. 2) was controlled by changing

the level of the water which was used as the test liquid. A second baffle was used during certain pressure and damping studies to determine the effects of baffle separation. For the baffle-separation tests, the second baffle was installed at various preselected distances from the fixed top baffle.

Instrumentation

To obtain the differential pressure exerted on the top baffle, a system utilizing two strain-gage differential-pressure transducers (flat response from 0 to 700 hertz) was installed. These transducers were sealed from the water and positioned on the baffle as shown in figure 3. The individual output signals from these transducers were amplified and summed (polarity being opposite) to yield a signal which was proportional to the difference in pressure across the thickness of the baffle. The constant of proportionality for each transducer was obtained prior to filling the tank, in a static calibration in which the pressure was read directly from a manometer. During testing the transducer signal was recorded (flat response from 0 to 90 hertz) as an oscillogram.

Tests were conducted to determine whether significant interference effects resulted from the close proximity of the transducer housing of one gage to the pressure field of the diaphragm of the opposite gage. Recordings of the output of a single gage with and without the presence of the opposite transducer housing indicated that significant interference effects were not present over the range of fluid velocities and amplitudes studied in the present investigation.

The displacement amplitudes of the liquid in the test tank were also sensed by a strain-gage differential-pressure transducer (flat response from 0 to 700 hertz) which was sealed in a 1.91-cm-diameter tube open to the atmosphere as shown in figure 4. The sensing element was placed a fixed distance below the quiescent surface at the location of the liquid antinode ($\beta = 0^{o}$). The amplitude of the output signal was directly proportional to the liquid amplitude, the constant of proportionality being determined in a separate calibration in which the liquid amplitude was read directly from a scale along the tank wall. The transducer signal was recorded (flat response from 0 to 90 hertz) as an oscillogram. Both the displacement amplitude and damping of the liquid oscillations were determined from this record.

Procedure

The test procedure was essentially the same for both single and multiple baffle systems. Prior to each test the baffles were spaced according to the individual test requirements. The baffle spacing s/W ranged from 0.5 to 2.0, in increments of 0.5, for these tests. The tank was filled to a selected level with respect to the top baffle (d/r), which for these tests ranged from -0.1 to 0.4. The liquid was then excited in the fundamental

antisymmetric mode by manually applying a vertical excitation at the fundamental slosh antinode with a plunger opposite the pressure measuring system. (See fig. 1(b).) When the displacement amplitude ζ of the liquid surface reached the highest attainable value, the plunger was removed. Differential-pressure data, measured on the upper baffle only, were obtained from the record during both buildup and decay, whereas the slosh damping data were obtained by measuring the free decay of the liquid only.

DATA REDUCTION AND ANALYSIS

Baffle Pressures

The measured pressure data are presented in terms of a reduced velocity parameter which is a nondimensional parameter (often referred to as the period parameter) describing the relative velocity conditions of the liquid in the vicinity of the baffle. The reduced velocity parameter may be written as

$$\frac{U_{max}T}{2W} \tag{1}$$

where U_{max} is the maximum liquid velocity at the baffle location, T is the natural period of the oscillation, and W is the baffle width. The reduced velocity parameter was shown in reference 8 to be similar to the Strouhal number and to be important in correlating drag coefficients of plates in an oscillating flow. From reference 5 the maximum vertical velocity in a cylindrical tank at the baffle location due to the antisymmetric mode, as obtained from a potential solution (no baffle), may be written

$$U_{max} = \omega\zeta_{max}\frac{\sinh\left(1.84\frac{h-d}{r}\right)}{\sinh\left(1.84\frac{h}{r}\right)} \tag{2}$$

where ω is the natural slosh frequency, ζ_{max} is the maximum displacement amplitude at the surface, d is the distance of the baffle below the quiescent surface, r is the tank radius, and h is the liquid depth. When the baffle is located at or below the quiescent surface, the value of U_{max} obtained from equation (2) at the baffle depth may be used in equation (1) to obtain the value of the reduced velocity parameter.

When the baffle is above the quiescent surface, the velocity U_{max} at the baffle is less than the velocity $\omega\zeta_{max}$ at the liquid surface, and may be written as

$$U_{max} = \omega\zeta_{max}\cos\omega t \tag{3}$$

The angular displacement ωt is obtained from the relationship

$$d = \zeta_{max} \sin \omega t \tag{4}$$

where d is the distance of the baffle above the liquid surface. The relationship between the actual wave height and the reduced velocity parameter $U_{max}T/2W$ for the exposed and the submerged baffle is shown in figure 5.

The measured pressure data are nondimensionalized by dividing by the theoretical dynamic pressure $\frac{1}{2}\rho U_{max}^2$ and are compared with the theories presented in the NASA monograph "Propellant Slosh Loads" (ref. 6) and the theory presented by Davis in the appendix of the present paper. As given in reference 6, the maximum pressure acting on a submerged baffle subjected to the oscillatory velocity of sloshing liquid can be computed from the expression

$$P = K\rho U_{max}^2 \tag{5}$$

where K is the nondimensional parameter determined by Keulegan and Carpenter (ref. 8) and shown in figure 6.

When the baffle is above the quiescent liquid surface and subjected to the slapping action of the sloshing wave, an expression for the pressure of the form

$$P = 2\rho U_{max}^2 \tag{6}$$

is suggested in reference 6. This expression is based on impulse momentum and assumes that the velocity of the liquid is completely reversed when it strikes the baffle.

Frank C. Liu developed a theory for pressure of the form

$$P = 2\omega^2\rho\zeta e^{-3.68d/2r_W}\sqrt{1 - (y/W)^2} \sin \omega t \cos \beta \tag{7}$$

which is based on liquid acceleration about the baffle. (See refs. 1 and 7.) The expression also includes terms for radial and circumferential loading, y and β, respectively.

Davis (see appendix) derived a semitheoretical expression for pressure which includes both the liquid acceleration (as does Liu's expression) and liquid velocity. The expression, which is based upon an irrotational flow analysis and the experimental results of Keulegan and Carpenter, is

$$P = 2\rho\omega^2\zeta \frac{\sinh\left(3.68 \frac{h - d}{2r}\right)}{\sinh\left(3.68 \frac{h}{2r}\right)} \sqrt{W^2 - y^2} \sin \omega t \cos \beta$$

$$- \frac{3}{4} C_d \rho \left[\frac{\sinh\left(3.68 \frac{h - d}{2r}\right)}{\sinh\left(3.68 \frac{h}{2r}\right)}\right]^2 \omega^2 \zeta^2 \left(1 - \frac{y^2}{W^2}\right) \left|\cos \omega t\right| \cos \omega t \cos^2 \beta \tag{8}$$

The analysis also includes the terms for radial and circumferential loading. The drag coefficient C_d is discussed in the appendix and is assumed to be

$$C_d = 15\left(\frac{U_{max} T}{W}\right)^{-1/2} \tag{9}$$

Slosh Damping

The damping data are presented in terms of the logarithmic decrement, defined as

$$\delta = \frac{1}{N} \log_e \frac{\zeta_n}{\zeta_{N+n}} \tag{10}$$

where N is the number of cycles occurring over the amplitude range of ζ_n to ζ_{N+n}. When applicable, these data were compared with the theoretical values determined from the relationship of Miles, reference 5:

$$\delta = 2\pi \, 2.83 e^{-4.60 d/r} a^{3/2} (\zeta/r)^{1/2} \tag{11}$$

where a is the fractional part of the cross-sectional area of the tank blocked by the baffle:

$$a = \frac{r^2 - (r - W)^2}{r^2} \tag{12}$$

RESULTS AND DISCUSSION

The test program consisted of the isolation and examination of the baffle pressure loads and slosh damping, with the following as variables: nondimensional liquid velocity

$U_{max}T/2W$, liquid amplitude ζ/r, baffle depth d/r, radial position on the baffle y/W, circumferential position β, and baffle spacing s/W. The dependence of the pressure loads on each of these variables is illustrated with representative data obtained with one and two baffles mounted in the tank, followed by damping data obtained with single and multiple baffles. These data are compared with available theories where applicable.

Baffle Pressure Loads

Effect of amplitude.- Sample data are presented in figure 7 to illustrate the effect of slosh amplitude, in terms of the nondimensional velocity parameter $U_{max}T/2W$, on the baffle pressure P. Pressures shown were measured at the antinode of the fundamental slosh mode ($\beta = 0^o$) and a radial position y/W of 0.25. Baffle depths d/r of 0.4 and -0.1 are presented to show the effect for both a submerged and an exposed (splash) baffle. (The negative value of d/r indicates that the baffle is above the quiescent surface.) Higher values of the velocity parameter are presented for $d/r = -0.1$ because of the ease of manually exciting much larger slosh amplitudes when there is no baffle below the quiescent liquid surface. Theoretical values for submerged baffles included in the figure, obtained from Davis (appendix) and from reference 6 (eq. (5) of present paper), are derived for a submerged baffle subjected to oscillatory liquid flow. Theoretical values derived from Liu's equation (eq. (7)) are considerably lower than those of Davis for the range of depths and liquid velocities examined during these tests and therefore are not presented. Also included in figure 7 are theoretical values from reference 6 (eq. (6) of present paper) derived for the case in which the baffle is above the quiescent surface and subjected to a periodic slapping (splash) action of the sloshing wave. As might be expected, the pressure on the baffle increases with increasing values of the velocity parameter. Furthermore, there appears to be good agreement between theoretical and experimental results for the submerged baffle and fair agreement when the baffle is exposed.

Figure 8 shows the effect of slosh amplitude, in terms of the nondimensional velocity parameter $U_{max}T/2W$, on the nondimensional baffle pressure parameter $P/\frac{1}{2}\rho U_{max}^2$ for all experimental data. Pressures were measured at $\beta = 0^o$ for radial positions y/W of 0.25, 0.5, and 0.75 and baffle depths d/r ranging from 0.4 to -0.1. Although a baffle depth of 0.05 is below the quiescent surface, the baffle was generally exposed during some portion of the slosh cycle. It should be noted that the theoretical values for the submerged case are dependent on $U_{max}T/2W$ but independent of d/r, whereas the splash theory (ref. 6) when nondimensionalized is independent of $U_{max}T/2W$. The measured values of the pressure parameter decrease with increasing values of the velocity parameter in both submerged and exposed cases and also vary with baffle depth d/r between 0.1 and -0.1.

There appears to be good theoretical and experimental correlation when the baffle is relatively far below the liquid surface (submerged theory, d/r greater than 0.1) or well above the liquid surface (d/r of -0.05 and -0.1) and subjected to slosh of relatively high amplitude. Agreement is not quite as good, however, when the baffle is only slightly submerged or exposed, probably because of the greater liquid turbulence. At these shallow depths (d/r of 0.05, 0, and -0.05) the highest pressures were recorded for given values of $U_{max}T/2W$. This may or may not be the critical design condition, however, because of the high damping and, hence, low values of $U_{max}T/2W$ associated with these shallow depths. The critical design depth and velocity $U_{max}T/2W$ can be determined only from detailed analyses of vehicle stability and loads.

Effect of radial position.- Although the effect of radial position y/W on the baffle pressure parameter may be observed by reviewing all the data of figure 8, a summary of the effect is shown in figure 9. The distribution of the pressure in terms of y/W is presented for liquid depths d/r of 0.2 and 0.4. The experimental distributions are compared with the theory of Davis, which includes the pressure distribution across the baffle, and with the theoretical values from reference 6 (eq. (5) of present paper), which does not include y/W effects. Davis's prediction of the magnitude of the pressure across the baffle is somewhat low for a low value of $U_{max}T/2W$, but does follow the trend of the data.

Effect of circumferential position.- The effect of circumferential position β on the baffle pressure parameter is presented in terms of the nondimensional velocity parameter $U_{max}T/2W$ in figure 10. The data given were measured at a radial position y/W of 0.5 and at baffle depths d/r of 0 and 0.4. The theory of Davis is shown for comparison with the data taken at $d/r = 0.4$. Agreement appears to be good for $d/r = 0.4$ and $\beta = 30^{o}$, but as β increases the agreement is not as good. Although the theory predicts zero pressure at the nodal point ($\beta = 90^{o}$), the liquid in fact exhibits a vertical oscillatory component at the nodal point during antisymmetric slosh (see ref. 9, for example).

Effect of baffle spacing.- The effect of baffle spacing s/W on the baffle pressure parameter is presented in terms of the nondimensional velocity parameter $U_{max}T/2W$ in figure 11. The data were measured on the top baffle of the two-baffle system at the antinode position ($\beta = 0^{o}$) and radially at $y/W = 0.5$. Baffle depth d/r varied from 0.4 to 0. For comparison, faired curves based on the data for the single baffle are also presented. With the possible exception of the spacing s/W of 0.5, the addition of a second baffle provided little or no attenuation of the baffle pressures. In fact, under certain conditions the pressures were higher in the case of the multiple baffle.

Damping

Effect of amplitude.- The effect of surface amplitude ζ/r on damping is shown in figure 12. Damping values are presented for baffle spacings s/W ranging from 0.5 to 2.0. Baffle depth d/r varied from 0.4 to 0 and was measured from the quiescent surface to the top baffle. Damping data taken with a single baffle are also presented for comparison. Because of the common usage of Miles' theory (ref. 5), values were calculated by that theory for both single and multiple baffles ($s/W = 1$) and are presented in the figure. Although Miles' theory was derived for a single baffle, the theoretical value at $s/W = 1$ was calculated by taking the damping value of the second baffle at its given d/r and adding to it the damping value of the single baffle at its given d/r.

The data show higher damping for increasing surface amplitudes and decreasing depths, as would be expected. In general, the theoretical curve for the single baffle is about 20 percent higher than the experimental values for depths d/r ranging from 0.4 to 0.2. When the assumptions and approximations made in the derivation are considered, this agreement is considered good and is believed to be sufficiently accurate for most applications. For depths d/r of 0.1 or less, it is evident that agreement is not as good. This disagreement is probably due to the turbulent nature of the liquid in this region. The modified theory for the multiple-baffle damping ($s/W = 1$) predicts damping values higher than experimental values for baffle depths d/r of 0.4 to 0.1 and lower than experimental values for baffle depths below this level. This disparity between theory and experiment is caused by flow interference effects which decrease the independent effectiveness of each baffle. This may be seen from the experimental data alone. If the damping contributions of two independent single baffles at a spacing of $s/W = 1$ are combined, in all cases the multiple-baffle data are lower, a result which suggests flow interference.

Effect of baffle spacing.- The effect of baffle spacing s/W on damping is summarized in figure 13. Damping values are presented for a range of baffle depths d/r from 0 to 0.4 and for surface amplitudes ζ/r of 0.02 and 0.04. Damping data for a single baffle are also presented (value at $s/W = 0$). The data show that adding a second baffle to the system may either increase or decrease the total damping effectiveness, depending on the liquid depth and baffle spacing, but in general, for baffle depths of $d/r > 0.1$, little benefit is realized. Multiple baffles are required, of course, to provide damping as the liquid drains from the tank. Therefore, the final design of a baffle system for a tank with changing liquid depths must be optimized in terms of damping requirements and practical considerations such as weight, strength, and cost.

CONCLUSIONS

An investigation was conducted to determine the liquid pressure loads and slosh damping associated with rigid ring baffles in relatively large cylindrical tanks. Results

suggest that liquid pressure distributions and slosh damping values can be determined from available theories for the design of single and multiple baffle configurations. The following specific comments are applicable in the range of variables covered by these tests:

1. Measured pressures are a function of the magnitude of the liquid velocity at the baffle location. In addition, pressures are dependent on the position of the baffle with respect to the free surface when the ratio of baffle depth d to tank radius r is less than 0.1.

2. The highest pressures measured for given wave heights and baffle depths occurred when the baffle was most effective as a slosh damper, near the quiescent surface of the liquid at a baffle depth d/r of 0.05.

3. The magnitude of the baffle pressure was not significantly affected by the presence of a second baffle located deeper in the tank.

4. When the baffle is submerged, theories based on oscillating flow about a submerged baffle (theories of Davis in present paper and of NASA SP-8009, "Propellant Slosh Loads") show excellent agreement with measured pressures. As the quiescent surface approaches the baffle position the agreement is not as good but is probably sufficient for most baffle designs. Furthermore, the trend of the radial and circumferential pressure distribution can be predicted by available theory.

5. When the baffle is exposed during a portion of the slosh cycle, the submerged-baffle theory predicts both the magnitude and the trend of the data with fair accuracy and appears to be better than the splash theory calculation from NASA SP-8009.

6. The magnitude of the damping resulting from the presence of a second baffle is less than would be obtained by adding the contributions of the individual baffles. Furthermore, when the baffles are closely spaced, the total damping may be less than that provided by a single baffle.

Langley Research Center,
National Aeronautics and Space Administration,
Hampton, Va., October 27, 1972.

APPENDIX

A SEMITHEORETICAL APPROXIMATION FOR RING-BAFFLE PRESSURE DUE TO LIQUID SLOSHING IN A CIRCULAR TANK*

Introduction

An entirely theoretical analysis that adequately describes the pressure forces on ring baffles seems thus far to have evaded researchers in the field. Nominal success has been achieved by assuming that the resulting flow around the baffle is irrotational. The irrotationality assumption may, at first, seem reasonable by virtue of the low viscosities of water and liquid propellants, but this is not the case. Since the prime purpose of the ring baffle is to dissipate mechanical energy, and since mechanical energy in fluids can be dissipated only through the action of viscosity, a completely irrotational flow model can hardly be expected to be adequate. That the flow is actually rotational is well known; for example, photographs of the eddies formed during the flow of water around plates similar to the ring baffle are shown in references 8 and 10. Since the nonlinearities inherent in the complete viscous (or inviscid) equations of motion governing the velocity field cannot be eliminated in problems of this type except when the flow is irrotational, an analytical treatment of baffle pressure problems is difficult. The only success in solving the complete equations of motion thus far has been with numerical techniques (ref. 11, for example) and, because of present computer capabilities, these solutions are usually limited to two-dimensional problems with relatively short time durations. However, there still remains the possibility of a more realistic approximate semitheoretical approach to the problem.

Frank C. Liu has demonstrated an analytical technique for determining the pressure force on a ring baffle due to irrotational sloshing. (See ref. 1.) Another inviscid analysis has been given by Armstrong and Kachigan (ref. 12). Garza (ref. 7) reported that his experimental results were in fair agreement with pressure loads predicted by these theories. However, pressure distributions predicted from completely irrotational flow models will be a function of the acceleration only. If rotational motion is involved, the pressure distribution will be a function of the velocity to some power as well as the acceleration. Since the velocity and acceleration are out of phase in sinusoidal motion, the maximum pressure on a baffle will appear at a different time during a cycle of motion than that predicted from inviscid theories; the excellent experimental work by Keulegan and Carpenter reported in 1958 (ref. 8) has shown this to be true.

---

*This work was accomplished by Phillip K. Davis as a participant in the ASEE-NASA summer faculty fellowship program at the Langley Research Center. He is presently Chairman of the Engineering Mechanics and Materials Department, Southern Illinois University, Carbondale, Illinois.

In this appendix the inadequacies of the completely irrotational flow model for describing the baffle pressure problem are discussed briefly. The irrotational flow model leads to a pressure distribution proportional to the fluid acceleration and independent of the velocity. Data from reference 8 are used to demonstrate that the maximum pressure on the baffle generally occurs at some time during a cycle of motion out of phase with both the velocity and the acceleration. The possibility of constructing a more realistic approximate semitheoretical analysis by using potential flow theory to obtain the baffle pressure distribution is discussed. Lastly, a semitheoretical expression for the baffle pressure, including both velocity and acceleration, is derived by combining the irrotational analysis and the experimental results of reference 8.

The Irrotational Flow Model

That there can be no net drag force acting on a body moving at constant velocity in an irrotational flow (the D'Alembert paradox) is well known in the field of hydrodynamics. However, there does exist a force resisting acceleration which is greater than the body's own inertia even in an inviscid fluid. The additional force is due to the inertia of a portion of the fluid medium surrounding the body whose motion is affected by the body. Problems of this type may be treated by first determining the proper amount to "increase" the mass of the body so that its resulting motion may then be determined by ignoring the fluid. For example, the "added mass" for a sphere is easily determined to be one-half the mass of the displaced volume of fluid by integrating the pressure, determined from potential-flow theory, over the surface of the sphere.

As a single example to demonstrate that the only pressure force acting on a body in motion in an irrotational fluid is nondissipative in nature, consider the equation governing simple pendulum motion of a sphere in water, which is considered to be an inviscid fluid:

$$\ddot{\theta} + \frac{g}{l}\left[\frac{(\text{sp. gr.}) - 1}{(\text{sp. gr.}) + \frac{1}{2}}\right]\theta = 0 \tag{A1}$$

where $\theta(t)$ is the angular displacement, l is the pendulum length, g is acceleration due to gravity, and sp. gr. is the specific gravity of the sphere. The resulting motion is not damped; in fact, the only effect of the fluid is to increase the period of oscillation. The pressure force difference across the sphere is maximum at the maximum value of $\ddot{\theta}$ (maximum acceleration) and zero for $\ddot{\theta} = 0$ (maximum velocity).

The first theoretical analysis of simple pendulum motion in a viscous liquid was accomplished by Stokes (ref. 13) in 1850. Stokes found a viscous component of drag proportional to the velocity as well as a component proportional to the acceleration. The

viscous component of the drag acts to dissipate the mechanical energy of the pendulum by damping the motion. Stokes also found that another effect of viscosity, in the pendulum problem, is to modify (increase) the added mass of the sphere from that predicted by the inviscid-flow analysis.

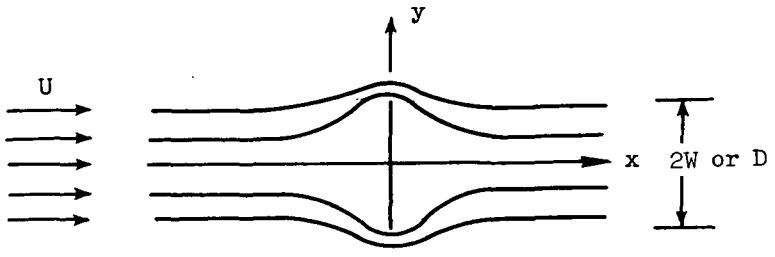

Sketch (a).- Steady irrotational flow around a plate.

The velocity potential for steady uniform flow impinging normally on a two-dimensional plate, as shown in sketch (a), may be obtained by the method of successive transformations:

$$w = U\sqrt{z^2 + (2W)^2} \tag{A2}$$

where w is the complex velocity potential,

$$w = \varphi + i\psi \tag{A3}$$

and z is the complex variable,

$$z = x + iy \tag{A4}$$

If the central streamline is imagined to be the tank wall, with the half-plate being the baffle, the resulting flow represents the irrotational flow around a ring baffle if the tank radius is large compared with the baffle width. Further, if U is allowed to be time dependent (unsteady) and a velocity $U(t)$ is then superposed on the entire system, directed in the negative x-direction, the result is equivalent to a plate traveling at $U(t)$ through an inviscid fluid otherwise at rest. By fixing a coordinate system to the plate and letting

$$U(t) = U_{max} \sin \omega t \tag{A5}$$

the pressure can be determined from

$$\frac{\partial \varphi}{\partial t} + \frac{\left|\frac{dw}{dz}\right|^2}{2} + \frac{P}{\rho} + \Omega = \text{Constant} \tag{A6}$$

where Ω is the body force potential function, provided $\partial\varphi/\partial t$ is determined correctly. Garza (ref. 7), by use of Liu's analysis (ref. 1), gives the resulting baffle pressure distribution as

$$P = -2\rho \frac{dU}{dt}\sqrt{W^2 - y^2} \tag{A7}$$

Integration of equation (A7) over the baffle gives the resulting force:

$$F = -2\left(\rho \frac{\pi W^2}{4}\right)\frac{dU}{dt} \tag{A8}$$

The added mass is two times the mass of liquid in a fictitious cylinder with diameter W. That this irrotational flow analysis yields both a pressure distribution and a net baffle force proportional to the acceleration is as expected. In the next section, experimental results are discussed which show the inadequacies of this model.

The Experiments of Keulegan and Carpenter

Underlying the experiments of Keulegan and Carpenter was the idea that the force on two-dimensional cylinders and plates in a sinusoidal flow could nearly be represented as the sum of a force component proportional to the velocity squared and a force proportional to the acceleration. Starting with the equation (ref. 8)

$$F = C_I \rho \frac{\pi D^2}{4} U_{max} \frac{2\pi}{T} \sin\frac{2\pi t}{T} - C_d \frac{\rho U_{max}^2}{2} D \left|\cos\frac{2\pi t}{T}\right| \cos\frac{2\pi t}{T} + \Delta R \frac{2\pi t}{T} \rho U_{max}^2 D \tag{A9}$$

they determined C_I and C_d from experimental data and found no correlation of these coefficients with the Reynolds number $U_{max}D/\nu$ over the range investigated $(5 \times 10^3 < U_{max}D/\nu < 14 \times 10^3)$, but instead found a definite relation of each to the period parameter (velocity parameter) $U_{max}T/D$. Further, they found ΔR to be negligible for low and high velocity parameters for cylinders, but more appreciable in the intermediate range of velocity parameters.* However, they report that the data for the plates

*They show comparison curves of measured F and the F calculated by neglecting ΔR for period parameters of 3 (low), 15.6 (intermediate), and 44.7 (high).

indicate that ΔR may not be disregarded, in particular when the velocity parameter is small.

It is apparent from equation (A9), especially when ΔR is negligible, that the inertia and drag components add in such a way that the maximum force occurs at some time during a cycle other than the times when either of them are separately a maximum. The following table shows the magnitudes of these forces for three values of the velocity parameter when $\rho = 9.99 \times 10^{-4}$ kg/cm^3, T = 2 sec, and D = 15.2 cm. The values of C_I, C_d, F_{max}, and the phase angle Φ are taken from reference 8. Also, equation (A9) was used with ΔR neglected for the calculations.

$\frac{U_{max}T}{D}$	U_{max}, cm/sec	C_I	C_d	$(F_I)_{max}$, N/cm	$(F_d)_{max}$, N/cm	$\frac{(F_d)_{max}}{(F_I)_{max}}$	F_{max}, N/cm	$\frac{(F_I)_{max}}{F_{max}}$	$\frac{(F_d)_{max}}{F_{max}}$	Φ, deg
2	15.2	1.60	10.8	130.16	177.61	1.37	214.22	0.61	0.83	24
2.5	19.0	1.67	10	169.48	257.61	1.52	306.41	.55	.84	25.6
5	38.1	2.30	7.24	466.40	740.28	1.59	881.28	.53	.83	32

How the separate forces add during a cycle of motion is shown in sketch (b). The sketch indicates the potential error involved in comparing a maximum load F (or pressure), measured experimentally, that occurs at one time during a cycle with a theory that predicts a maximum load at a different time during the cycle.

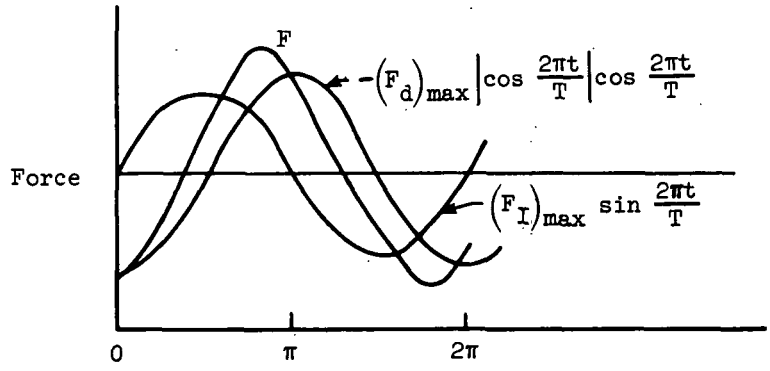

Sketch (b).- Comparison of force variations during a cycle.

An Approximate Semitheoretical Approach

The data of Keulegan and Carpenter are sufficient to show that, in general, a theory which predicts a baffle force proportional to the acceleration only is unrealistic. Experiments have established that energy-dissipating vortices are usually formed by the baffle.

For a velocity parameter of 1.6, the data in reference 10 indicate that eddies form, then break off, and are washed away along paths similar to those in sketch (c). This process suggests the possibility of developing an approximate semitheoretical analysis similar in

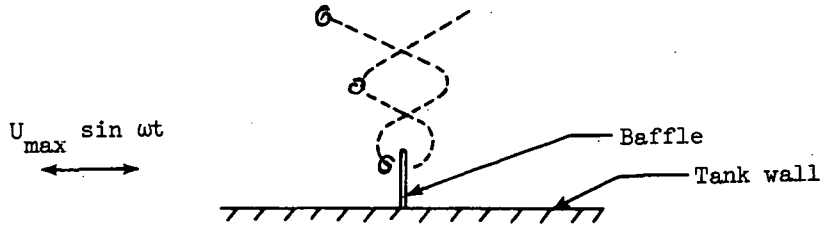

Sketch (c).- Vortex shedding from baffle at a velocity parameter of 1.6.

approach, perhaps, to that developed by Von Karman for the classical vortex sheet. Von Karman derived an approximate expression for the drag on a cylinder in motion at constant velocity in terms of the velocity of the cylinder, the velocity of the vortices, and the vortex spacing; however, resort must still be had to experiment to determine the period of vortex shedding and the vortex spacing in order to obtain numbers from the theory. The "added mass" pressure would arise naturally in an accelerative flow. This is not to imply that such an approximate analysis would be easy, even if possible. Also, Lamb (ref. 14, article 370) suggests that pressure distributions obtained from "potential" theories that yield a velocity-proportional drag may differ widely from actual pressure distributions.

Another approach leading to an approximate baffle pressure distribution is merely to add to the irrotational flow solution, equation (A7), a pressure component arising from the drag term. Such an expression can be determined from reference 8 by assuming a form of pressure distribution in the following manner. From the irrotational linear wave theory in reference 14, article 191, the velocity on the wall at depth d is

$$U = \omega\zeta \frac{\sinh\left(3.68 \frac{h - d}{2r}\right)}{\sinh\left(3.68 \frac{h}{2r}\right)} \cos \omega t \cos \beta \tag{A10}$$

where ζ is the slosh amplitude of the fundamental antisymmetric mode, d is the depth of the baffle below the surface, $2r$ is the tank diameter, h is the undisturbed depth of liquid in the tank, and β is an angle measured from the antinode position in the plane of the undisturbed free surface. Substitution of equation (A10) into equation (A7) gives

$$\left(P_{baffle}\right)_{inviscid} = 2\rho\omega^2\zeta \frac{\sinh\left(3.68 \frac{h - d}{2r}\right)}{\sinh\left(3.68 \frac{h}{2r}\right)} \sqrt{W^2 - y^2} \sin \omega t \cos \beta \tag{A11}$$

If a parabolic distribution of the following form is assumed:

$$(P_{baffle})_d = (P_d)_{max}\left(1 - \frac{y^2}{W^2}\right)\left|\cos \omega t\right|\cos \omega t \cos^2\beta \tag{A12}$$

a pressure distribution in terms of C_d can be determined from the expression for drag in reference 8 by integrating equation (A12). Future experimental results may indicate that another pressure distribution is more appropriate. The resulting pressure distribution is

$$(P_{baffle})_d = -\frac{3}{4} C_d \rho U_{max}^2\left(1 - \frac{y^2}{W^2}\right)\left|\cos \omega t\right|\cos \omega t \cos^2\beta \tag{A13}$$

where C_d (drag coefficient averaged over a cycle) is given graphically in figure 13 of reference 8 for a range of velocity parameters from 1.7 to 118.2. Miles (ref. 5) found that these data are given approximately by

$$\left.\begin{aligned} C_d &\approx 15\left(\frac{U_{max}T}{W}\right)^{-1/2} \qquad \left(2 \leqq \frac{U_{max}T}{W} \leqq 20\right) \\ \text{and} \qquad & \\ C_d &\approx 2 \qquad \left(\frac{U_{max}T}{W} \geqq 100\right) \end{aligned}\right\} \tag{A14}$$

Addition of equations (A11) and (A13) gives

$$P = 2\rho\omega^2\zeta \frac{\sinh\left(3.68 \frac{h - d}{2r}\right)}{\sinh\left(3.68 \frac{h}{2r}\right)}\sqrt{W^2 - y^2}\sin \omega t \cos \beta$$

$$- \frac{3}{4} C_d \rho\left[\frac{\sinh\left(3.68 \frac{h - d}{2r}\right)}{\sinh\left(3.68 \frac{h}{2r}\right)}\right]^2 \omega^2\zeta^2\left(1 - \frac{y^2}{W^2}\right)\left|\cos \omega t\right|\cos \omega t \cos^2\beta \tag{A15}$$

for the approximate baffle pressure distribution.

It is emphasized that expression (A15) depends on the following assumptions:

(a) That the net pressure may be represented as the sum of two pressures, one proportional to the acceleration and the other proportional to the velocity squared

(b) That the velocity-squared pressure distribution is approximately parabolic

(c) That the linear irrotational wave theory properly describes the motion in the immediate neighborhood of the baffle

However, this expression should be more appropriate than one based on a completely irrotational flow analysis. It is recognized that the inertia coefficient is a function of frequency or velocity parameter. The data of Keulegan and Carpenter show, however, that for sloshing configurations the values of the velocity parameter are relatively low and cover a narrow range, and therefore justification appears to exist for utilizing the derived constant value for the inertia coefficient.

REFERENCES

1. Silverman, Sandor; and Abramson, H. Norman: Damping of Liquid Motions and Lateral Sloshing. Ch. 4 of The Dynamic Behavior of Liquids in Moving Containers, H. Norman Abramson, ed., NASA SP-106, 1966, pp. 105-143.

2. Anon.: Slosh Suppression. NASA Space Vehicle Design Criteria (Structures). NASA SP-8031, 1969.

3. Silveira, Milton A.; Stephens, David G.; and Leonard, H. Wayne: An Experimental Investigation of the Damping of Liquid Oscillations in Cylindrical Tanks With Various Baffles. NASA TN D-715, 1961.

4. Stephens, David G.; and Scholl, Harland F.: Effectiveness of Flexible and Rigid Ring Baffles for Damping Liquid Oscillations in Large-Scale Cylindrical Tanks. NASA TN D-3878, 1967.

5. Miles, J. W.: Ring Damping of Free Surface Oscillations in a Circular Tank. J. Appl. Mech., vol. 25, no. 2, June 1958, pp. 274-276.

6. Anon.: Propellant Slosh Loads. NASA Space Vehicle Design Criteria (Structures). NASA SP-8009, 1968.

7. Garza, Luis R.: A Comparison of Theoretical and Experimental Pressures and Forces Acting on a Ring Baffle Under Sloshing Conditions. NASA CR-385, 1966.

8. Keulegan, Garbis H.; and Carpenter, Lloyd H.: Forces on Cylinders and Plates in an Oscillating Fluid. J. Res. Nat. Bur. Stand., vol. 60, no. 5, May 1958, pp. 423-440.

9. Abramson, H. Norman; Chu, Wen-Hwa; and Dodge, Franklin T.: Nonlinear Effects in Lateral Sloshing. Ch. 3 of The Dynamic Behavior of Liquids in Moving Containers, H. Norman Abramson, ed., NASA SP-106, 1966, pp. 79-103.

10. Schwind, Richard G.; Scotti, Richard S.; and Skogh, Jörgen: The Effect of Baffles on Tank Sloshing, Part I. LMSC-A642961 (Contract NAS1-4065), Lockheed Missiles & Space Co., Dec. 1964. (Available as NASA CR-67426.)

11. Welch, J. Eddie; Harlow, Francis H.; Shannon, John P.; and Daly, Bart J.: The MAC Method – A Computing Technique for Solving Viscous, Incompressible, Transient Fluid-Flow Problems Involving Free Surfaces. LA-3425, Los Alamos Sci. Lab., Univ. of California, Mar. 21, 1966.

12. Armstrong, G. L.; and Kachigan, K.: Stability and Control of Carrier Vehicles. Sec. 14.1 of Handbook of Astronautical Engineering, First ed., Heinz Hermann Koelle, ed., McGraw-Hill Book Co., Inc., 1961, pp. 14-2 – 14-53.

13. Stokes, G. G.: On the Effect of the Internal Friction of Fluids on the Motion of Pendulums. Trans. Cambridge Phil. Soc., vol. IX, pt. II, 1851, pp. 8-106.

14. Lamb, Horace: Hydrodynamics. Sixth ed., Cambridge Univ. Press, 1932.

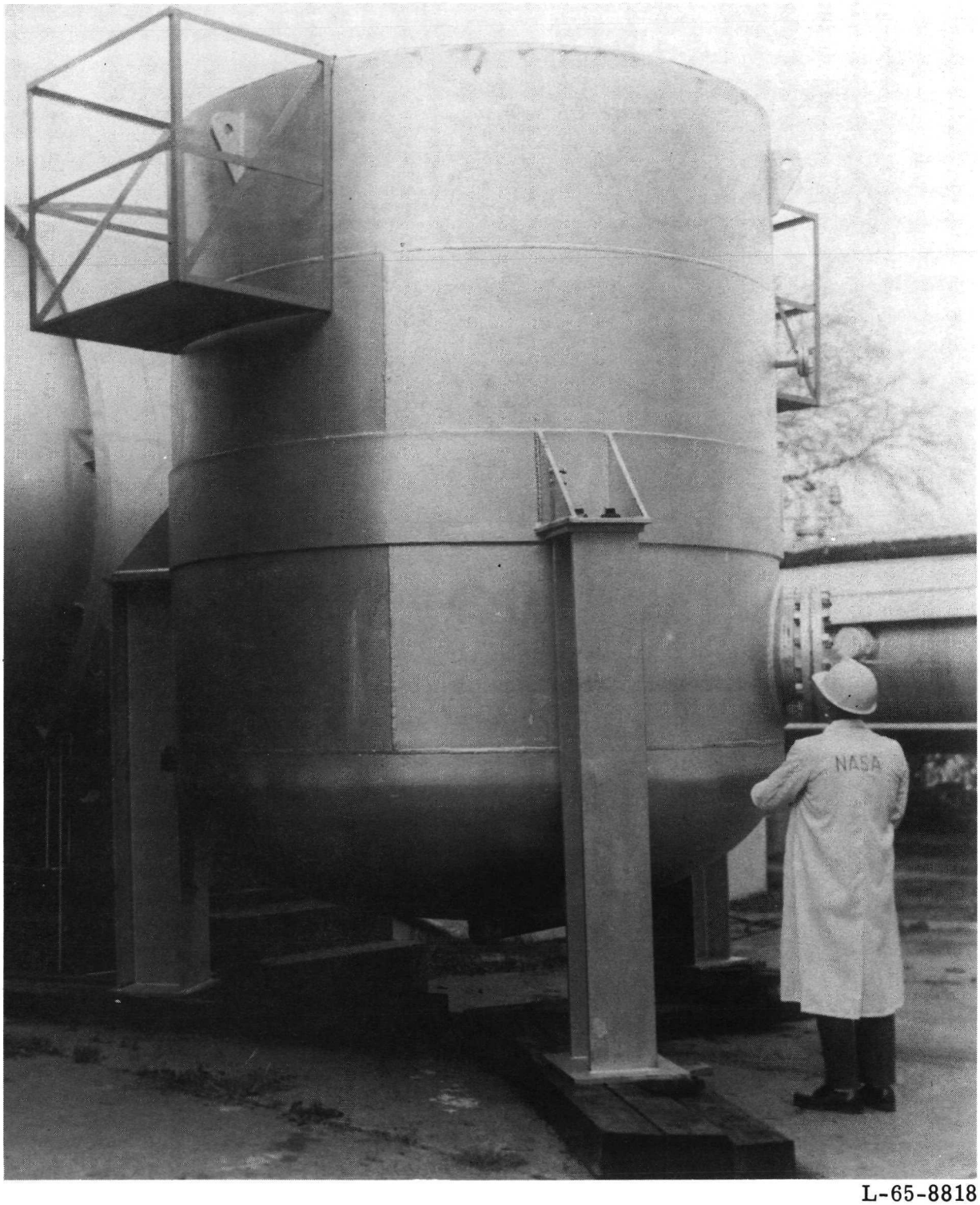

L-65-8818

(a) General view.

Figure 1.- Slosh tank with 284-cm diameter.

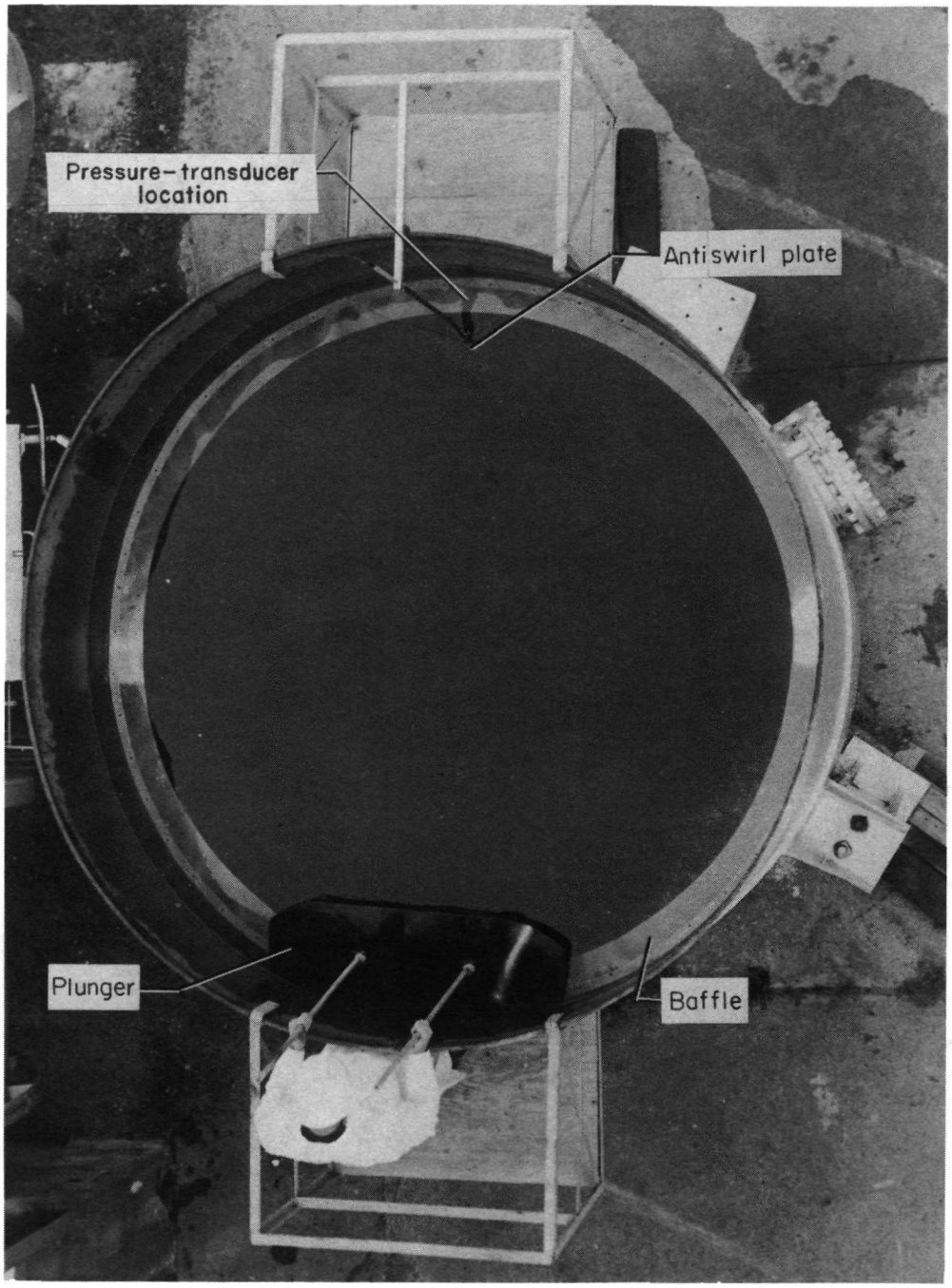

L-72-6554

(b) Plan view.

Figure 1.- Concluded.

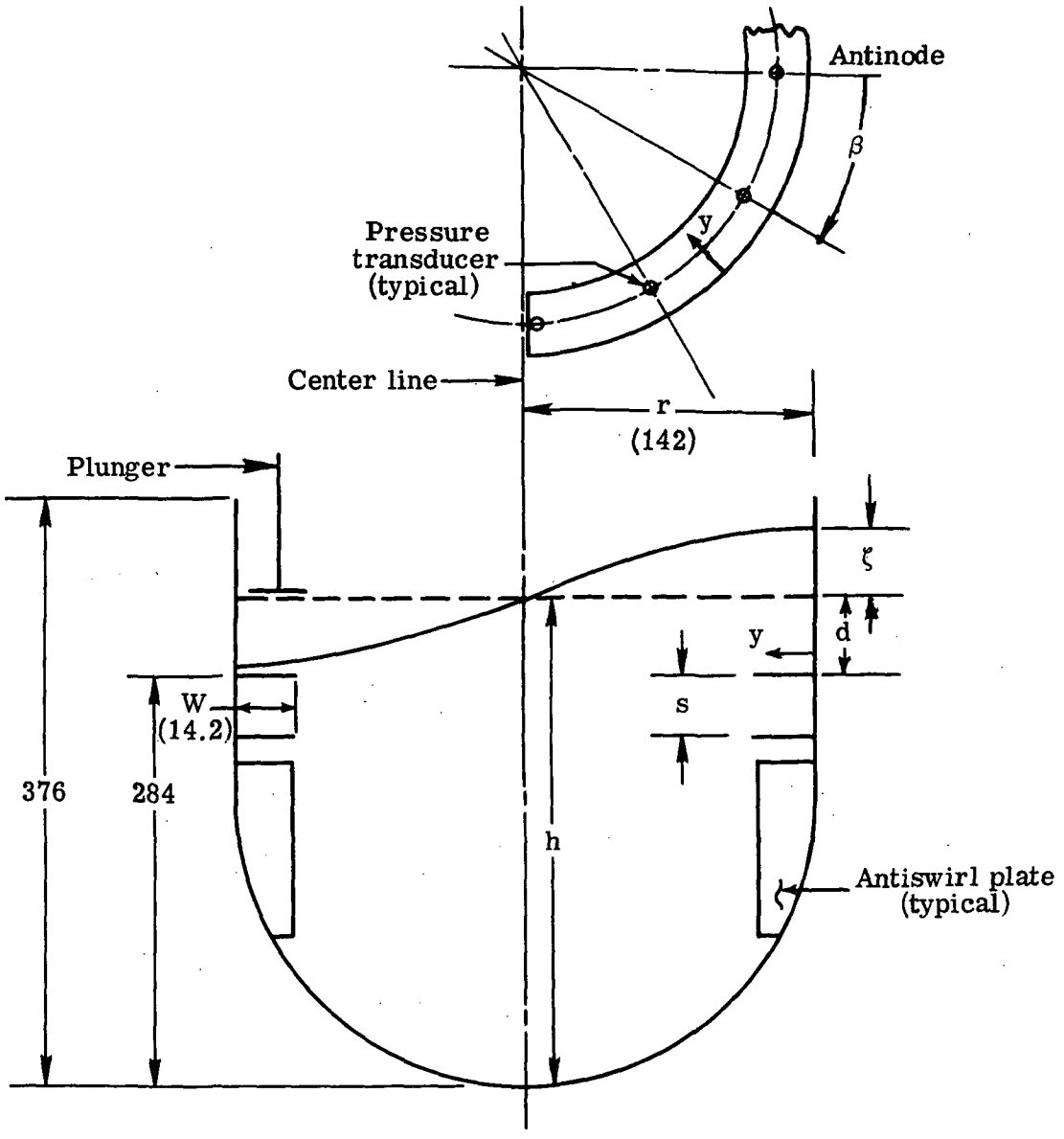

Test condition	d/r	s/W	y/W	β, deg
Single baffle	-0.1 to +0.4		0.25, 0.5, and 0.75	0 to 90
Two baffles	0 to 0.4	0.5 to 2.0	0.5	0

Figure 2.- Slosh-tank dimensions and test variables. Linear dimensions are in centimeters.

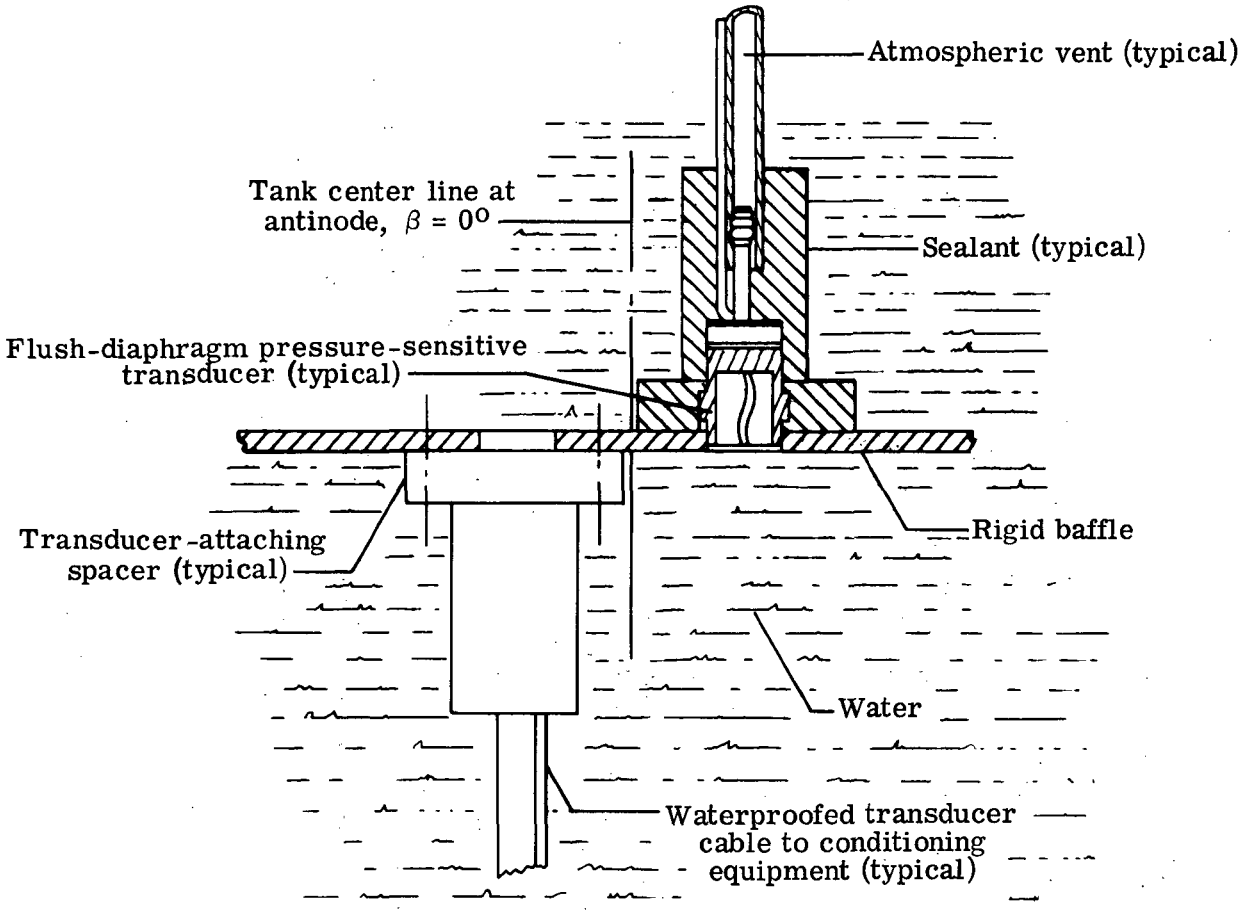

Figure 3.- Pressure-measuring system.

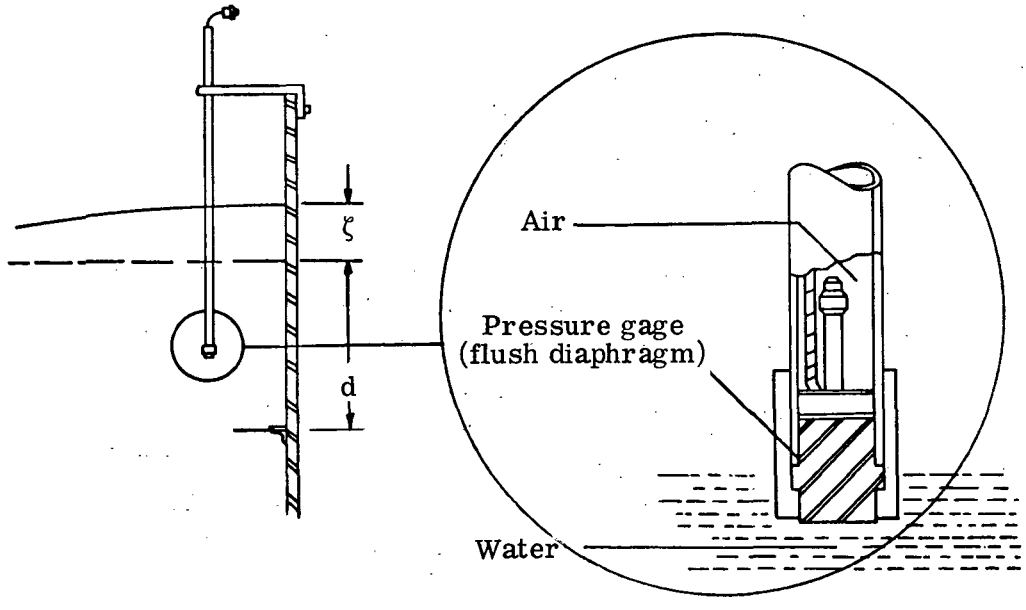

Figure 4.- Pressure-sensitive liquid-amplitude transducer.

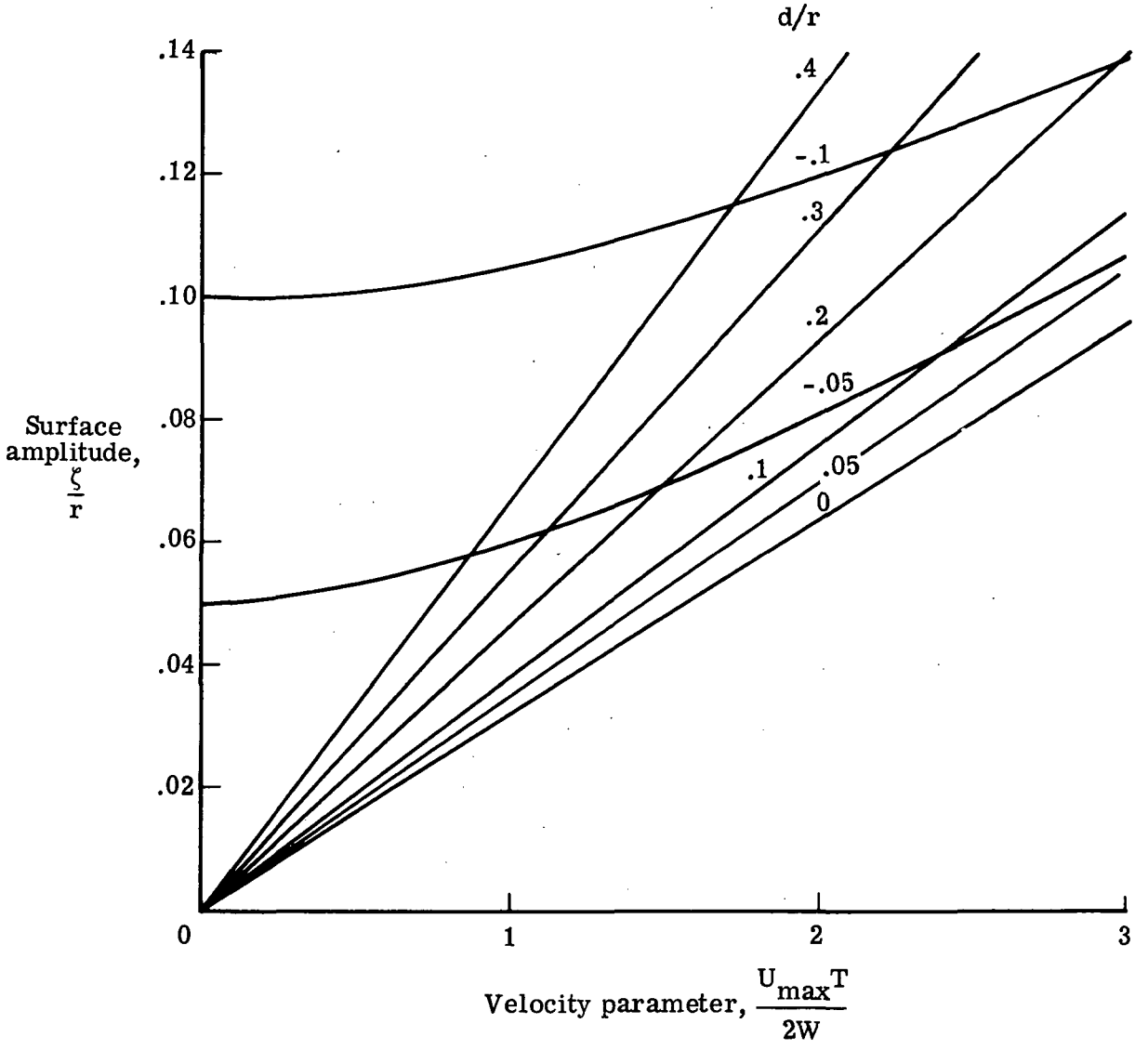

Figure 5.- Variation of surface amplitude with velocity parameter for various baffle depths.

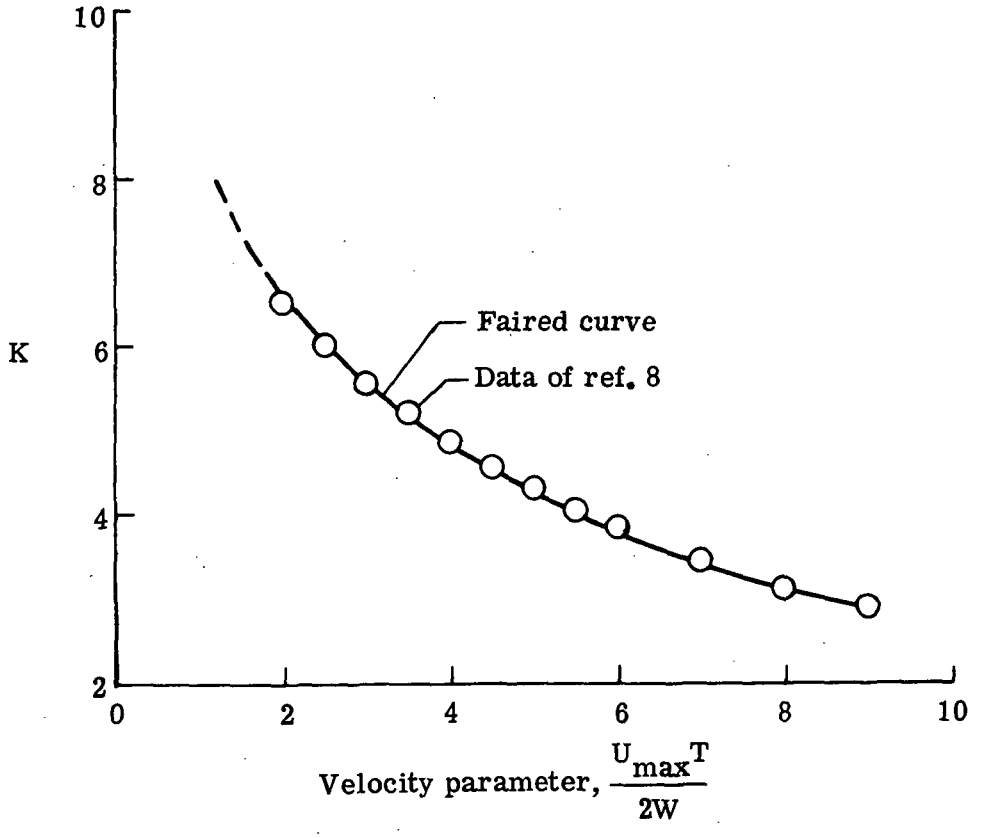

Figure 6.- Value of K for oscillating plates as given by Keulegan and Carpenter (fig. 32 of ref. 8).

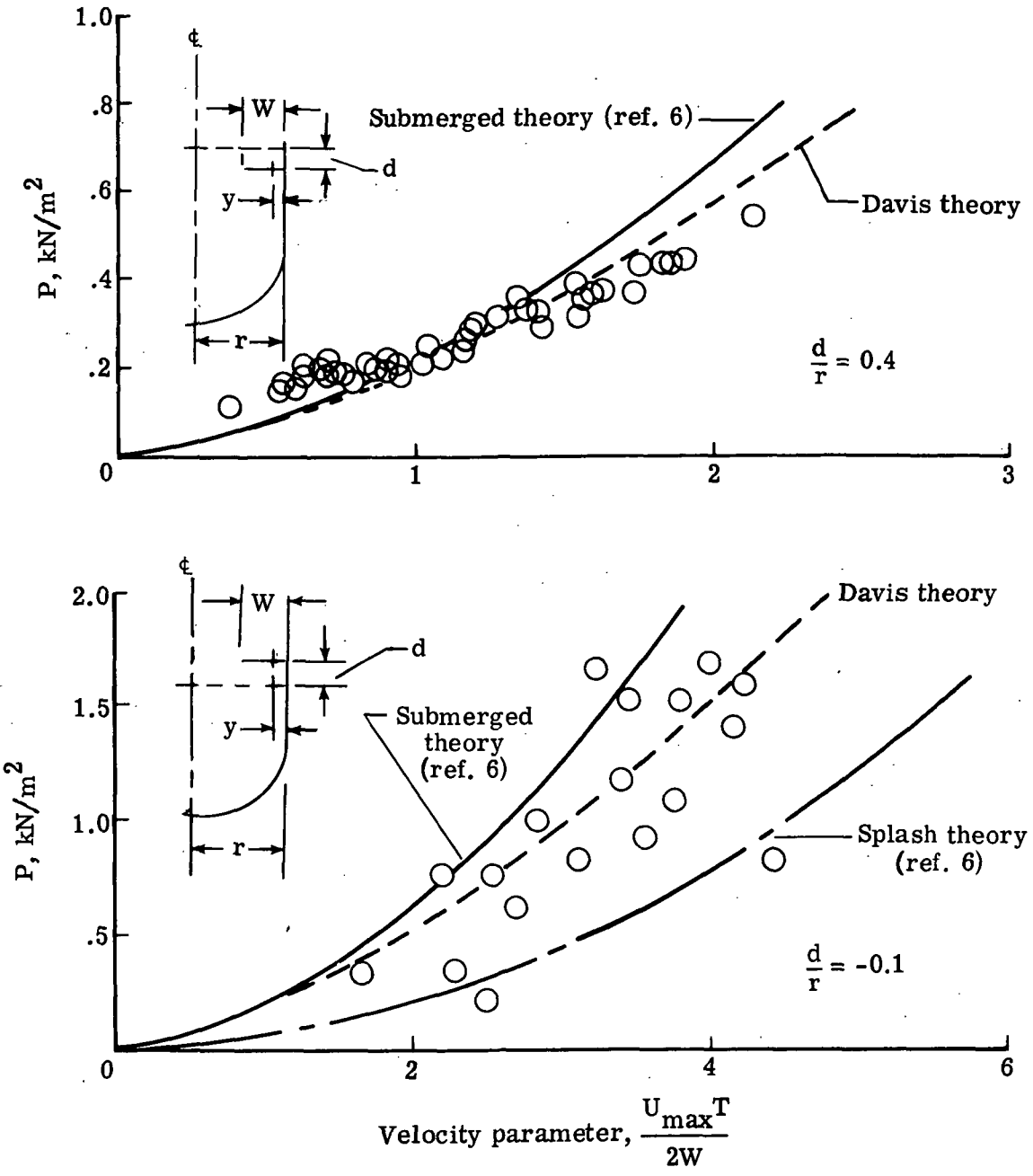

Figure 7.- Effect of velocity parameter on baffle pressure for two baffle depths. Single baffle; $\beta = 0^{o}$; y/W = 0.25.

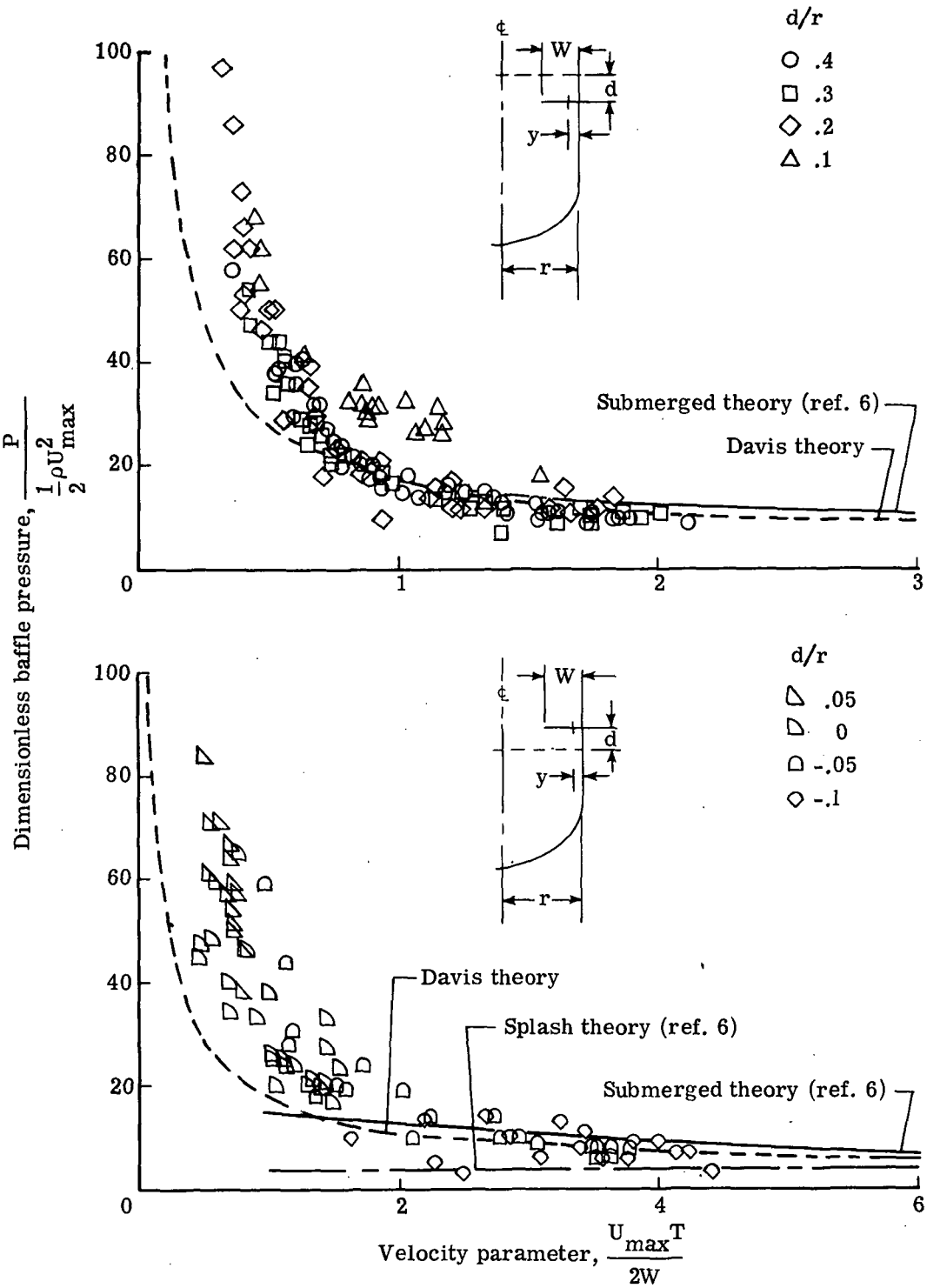

(a) y/W = 0.25.

Figure 8.- Effect of velocity parameter on baffle pressure parameter for a range of baffle depths. Single baffle; $\beta = 0^o$.

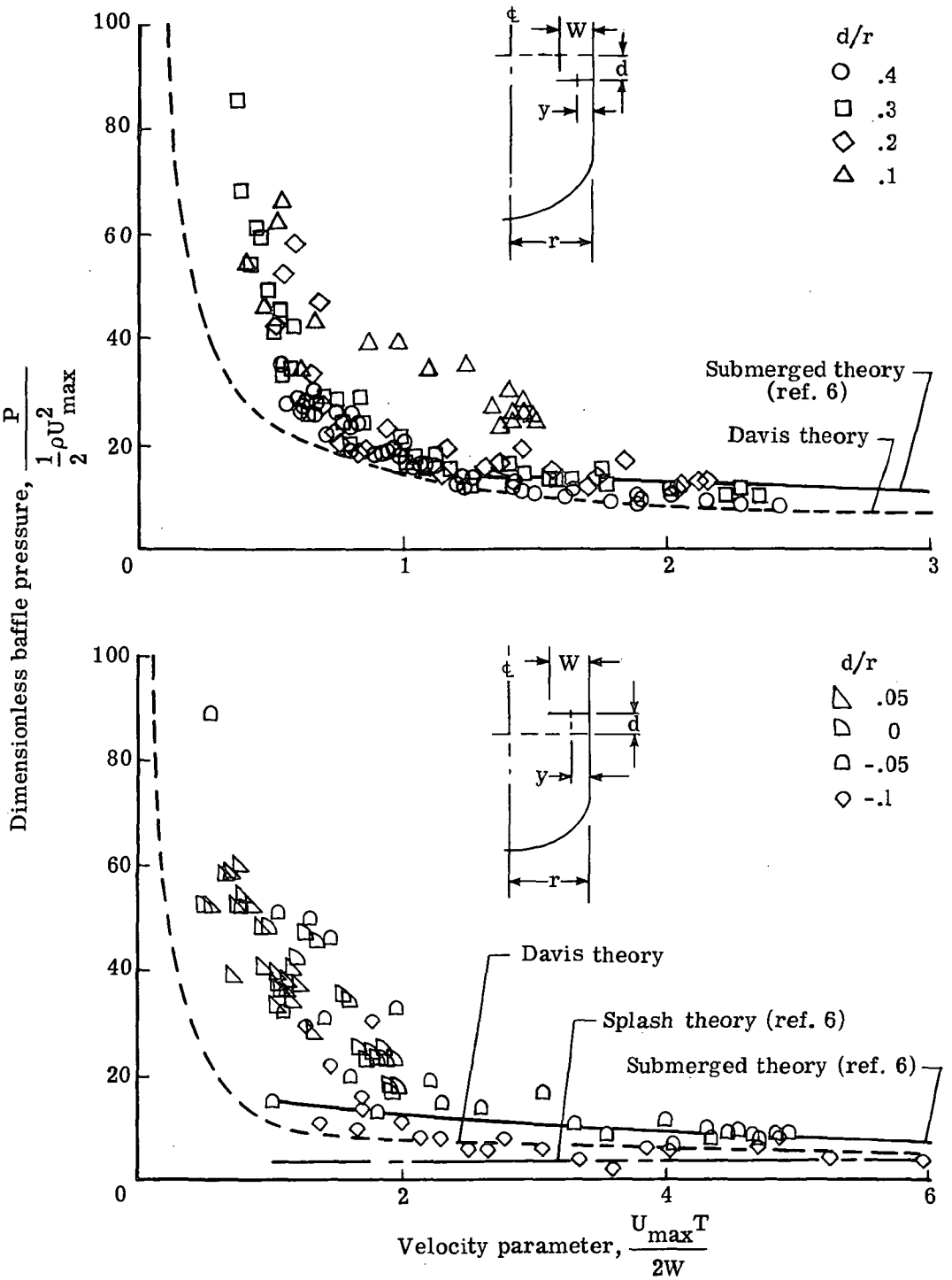

(b) y/W = 0.50.

Figure 8.- Continued.

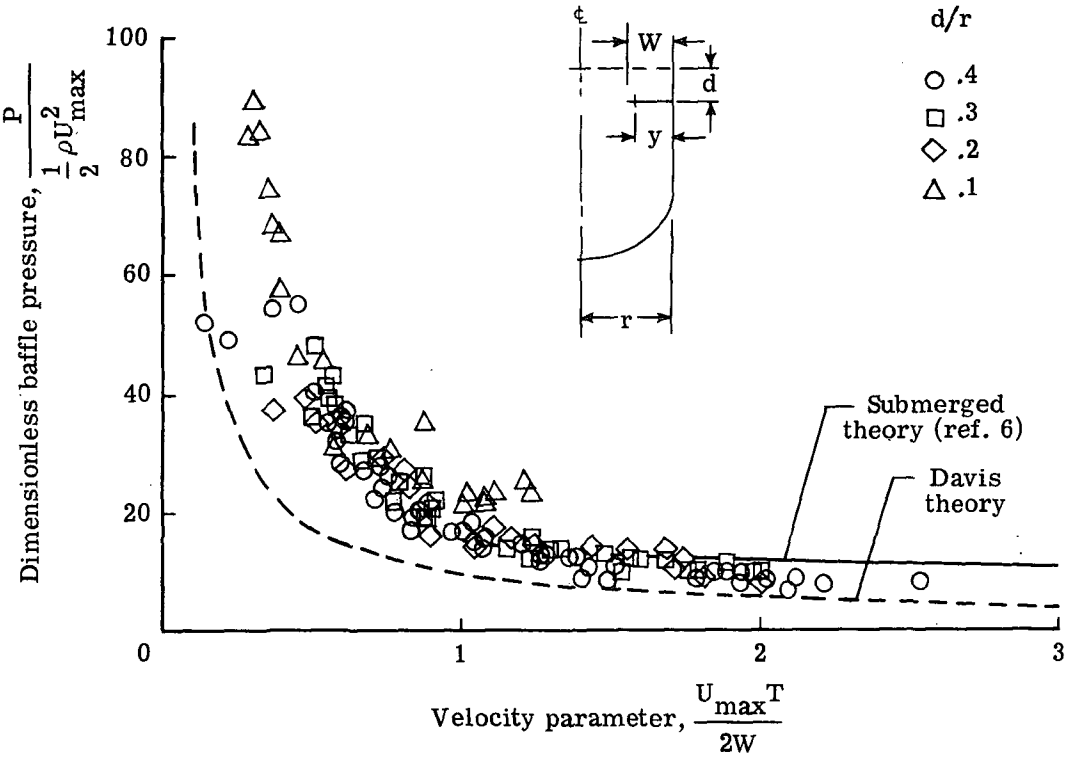

(c) y/W = 0.75.

Figure 8.- Concluded.

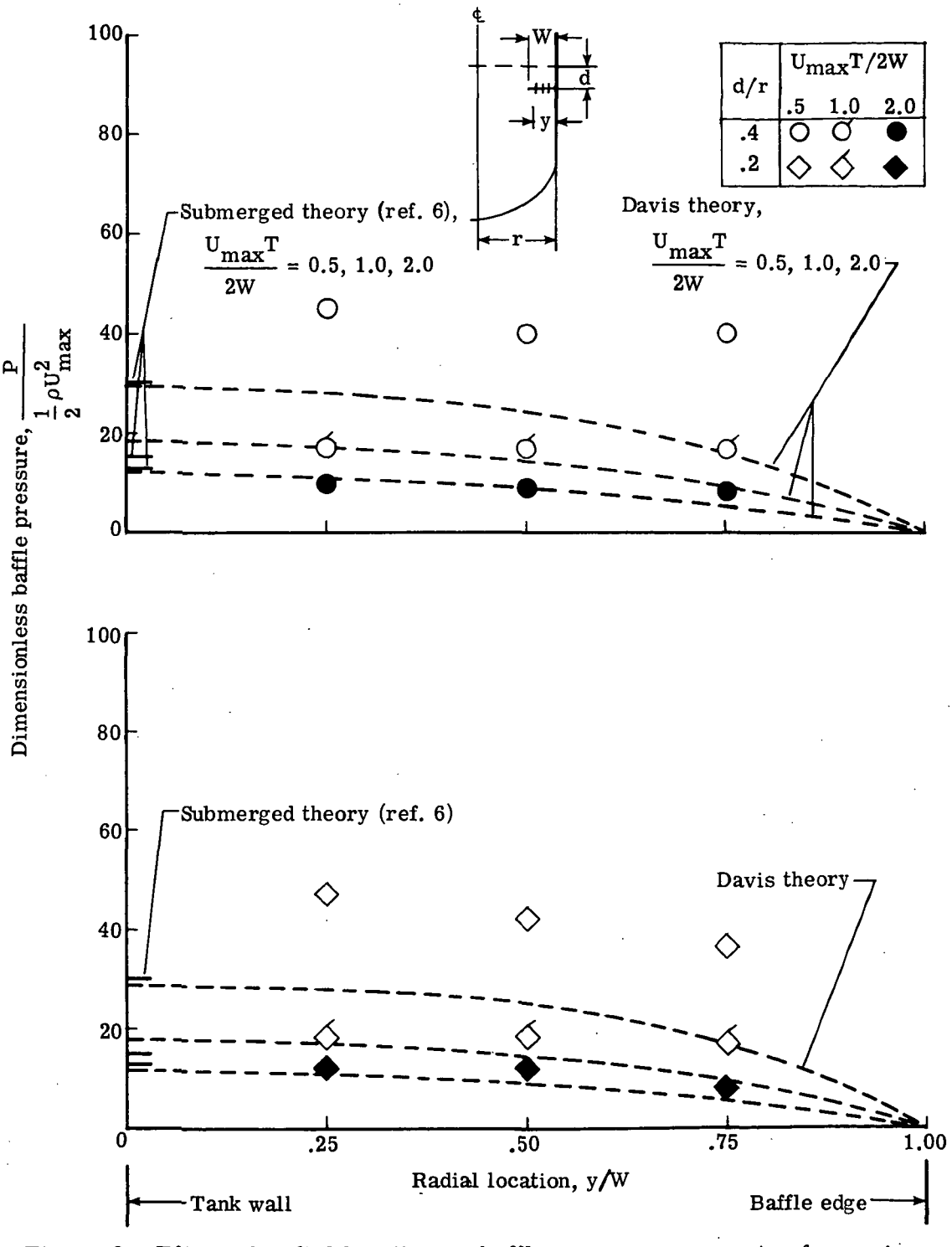

Figure 9.- Effect of radial location on baffle pressure parameter for various velocity parameters at two baffle depths. Single baffle; $\beta = 0^{o}$.

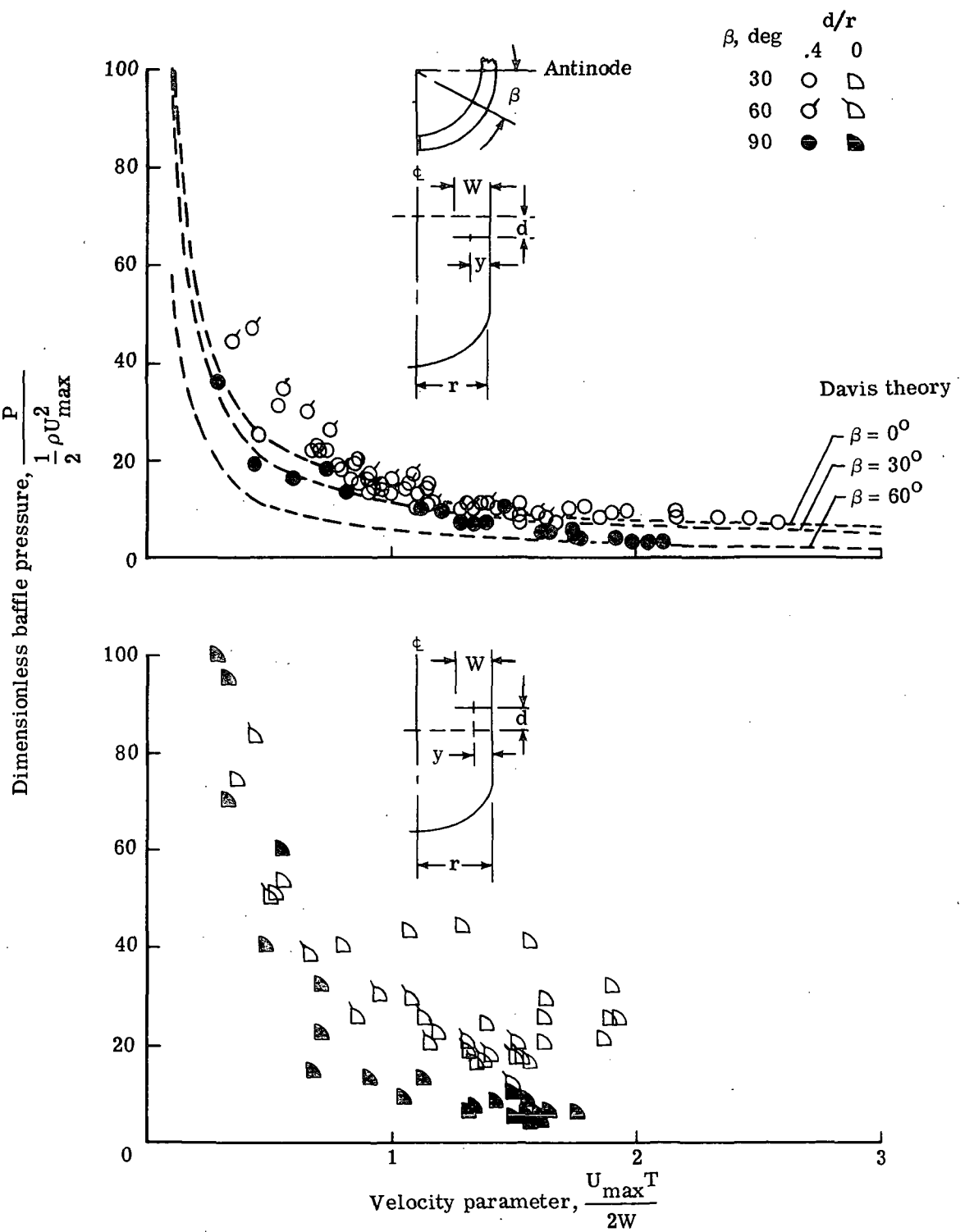

Figure 10.- Effect of velocity parameter on baffle pressure parameter for a range of circumferential locations at two baffle depths. Single baffle; y/W = 0.50.

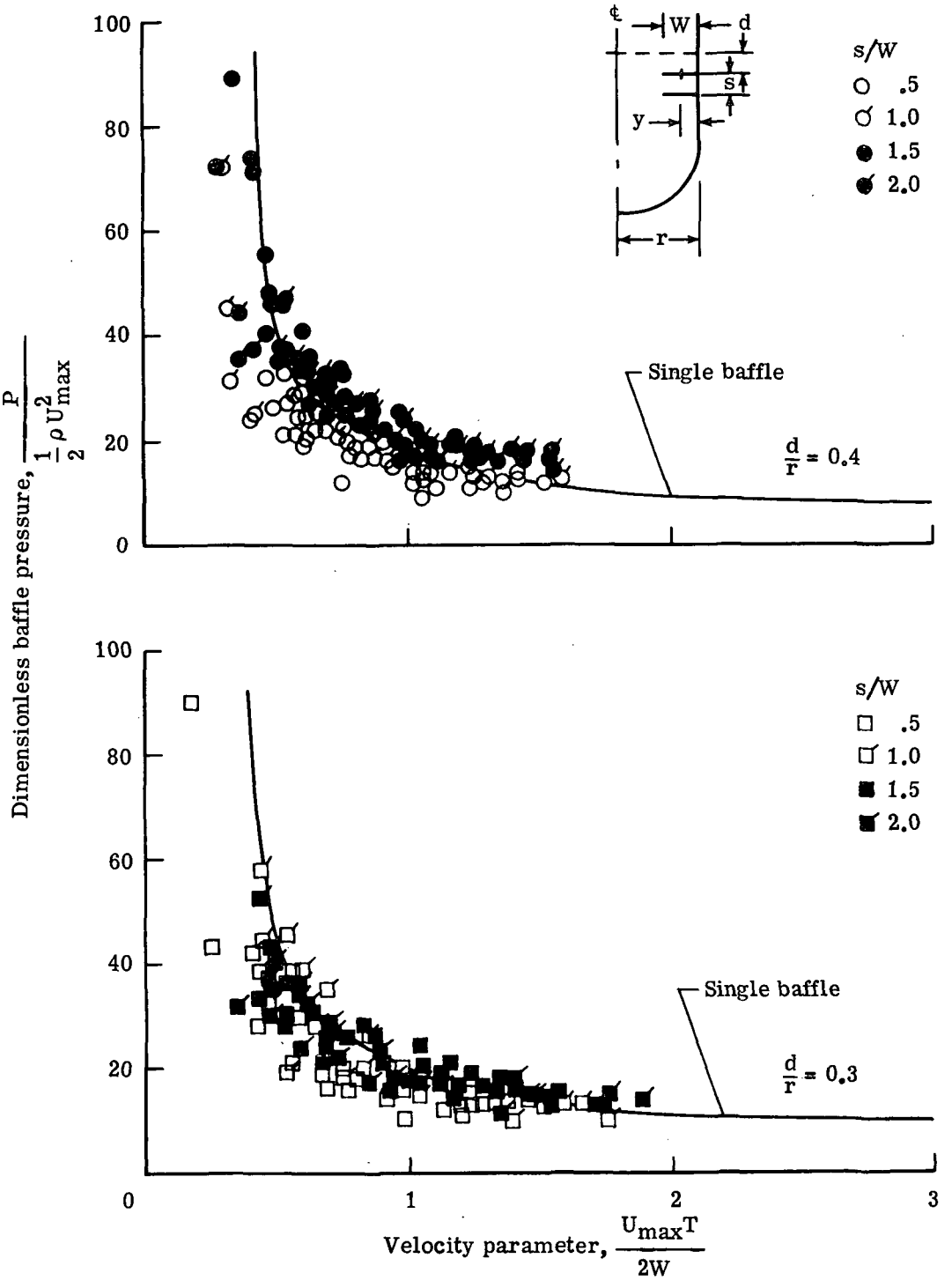

Figure 11.- Effect of velocity parameter on baffle pressure parameter for a range of baffle spacings and depths. $\beta = 0^{o}$; $y/W = 0.50$.

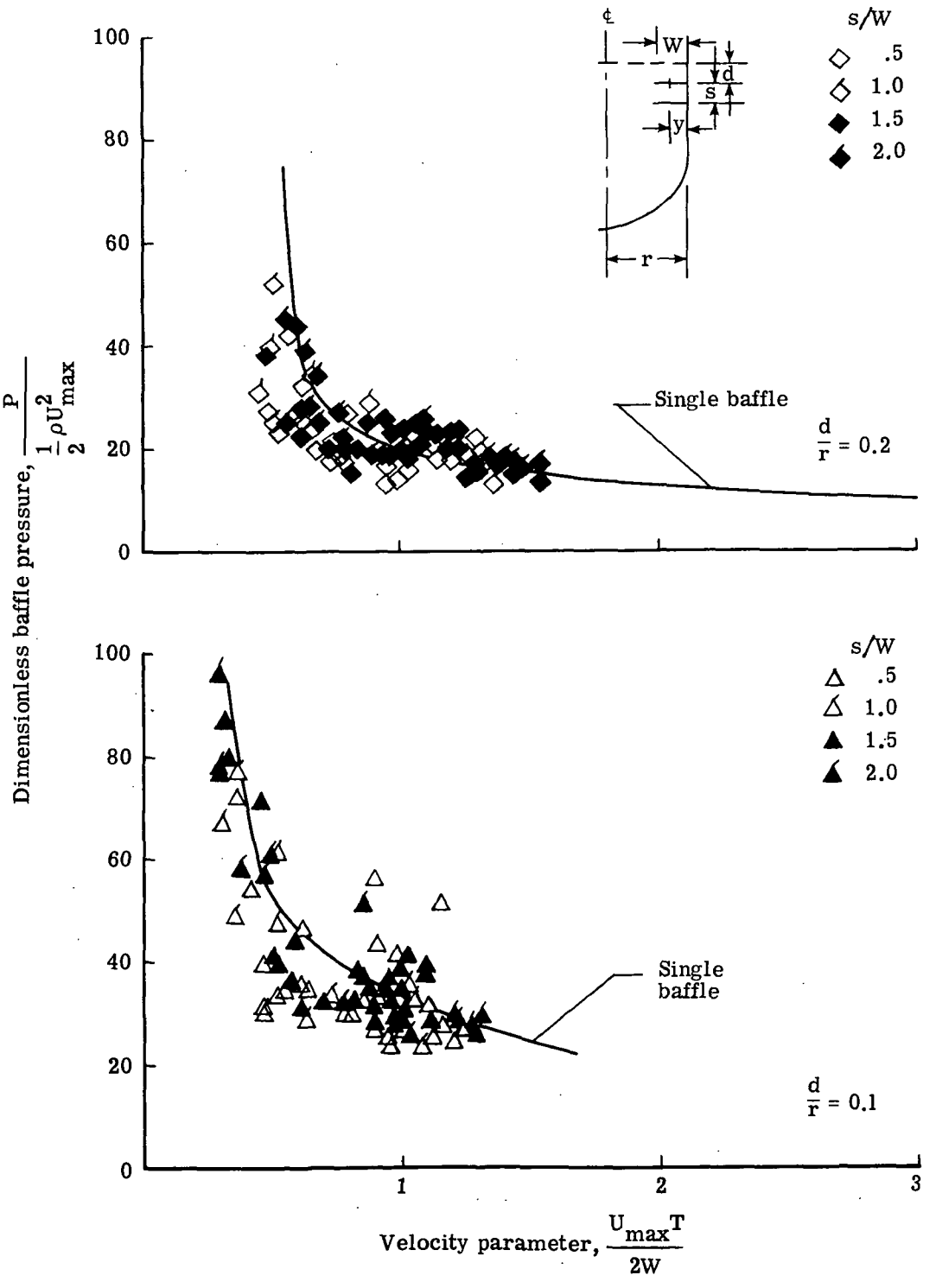

Figure 11.- Continued.

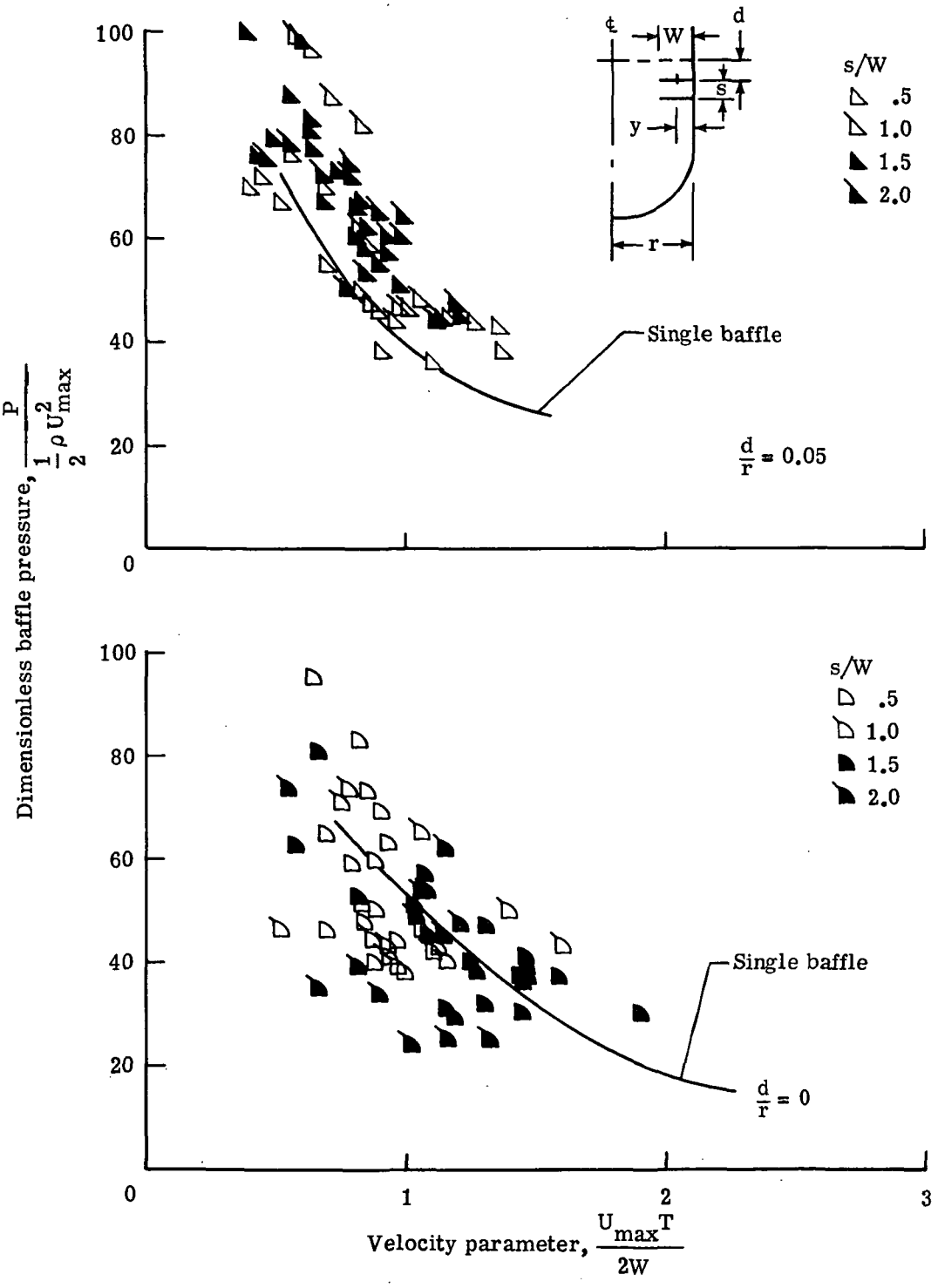

Figure 11.- Concluded.

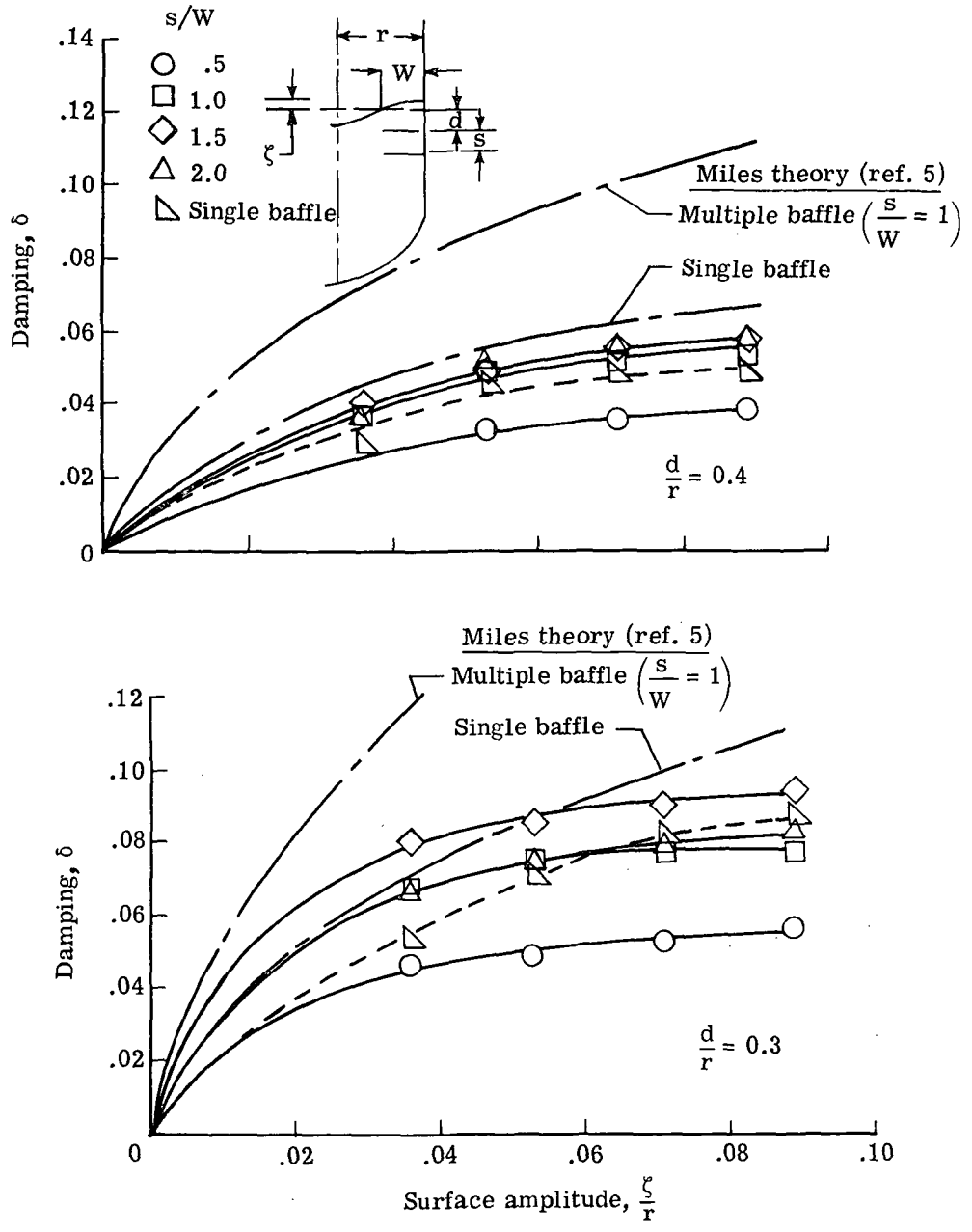

Figure 12.- Effect of surface amplitude on liquid damping for a range of baffle spacings and depths.

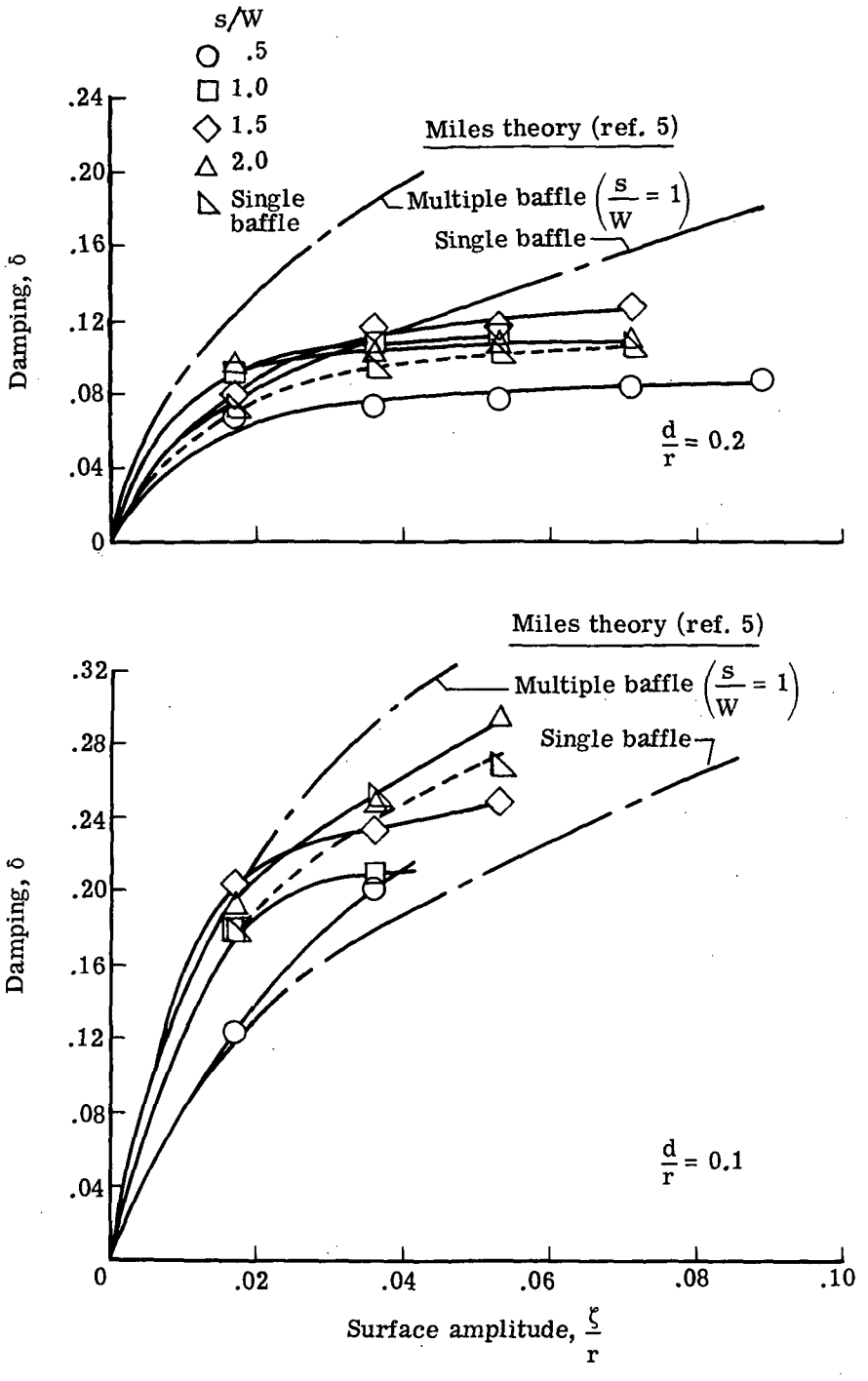

Figure 12.- Continued.

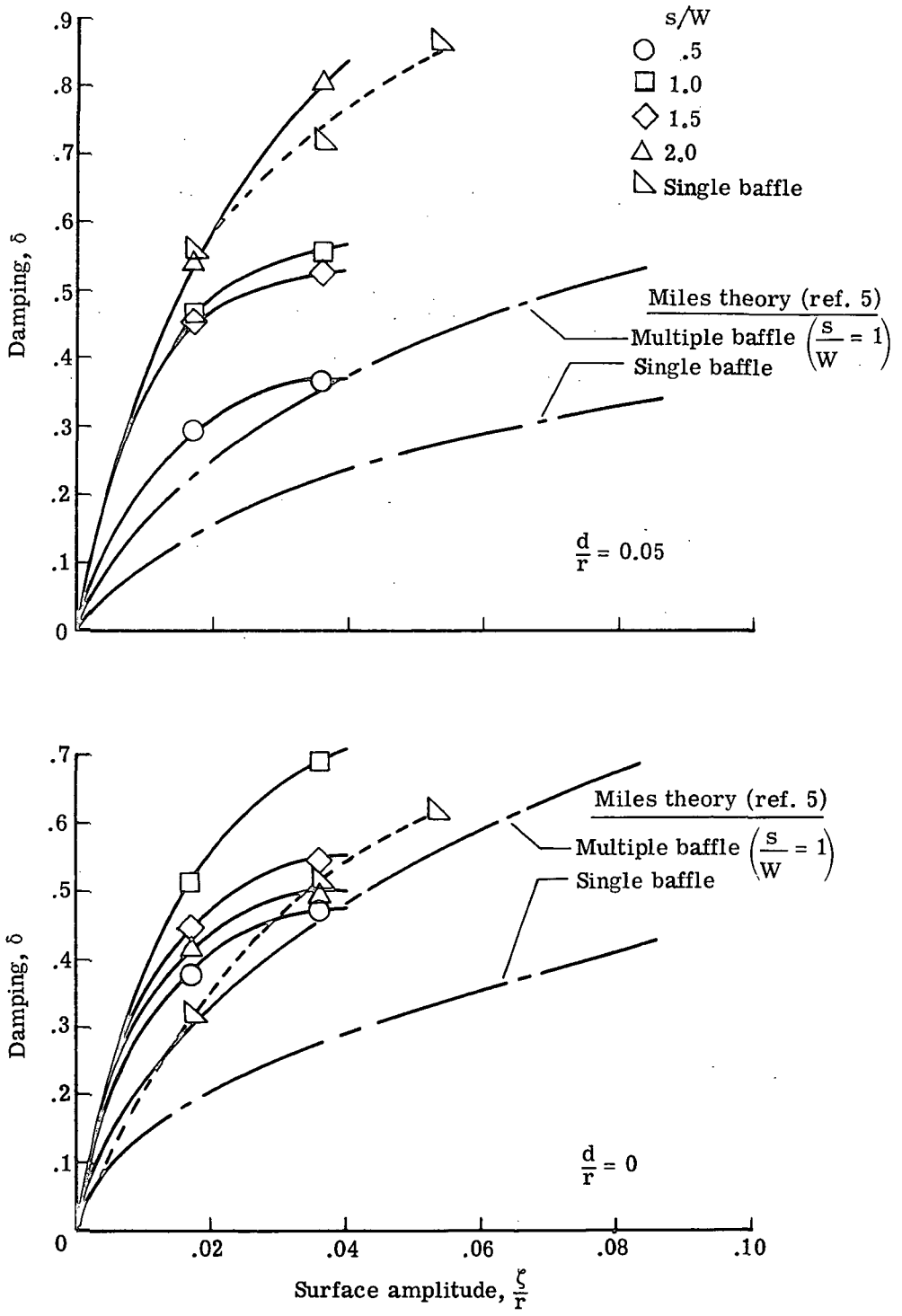

Figure 12.- Concluded.

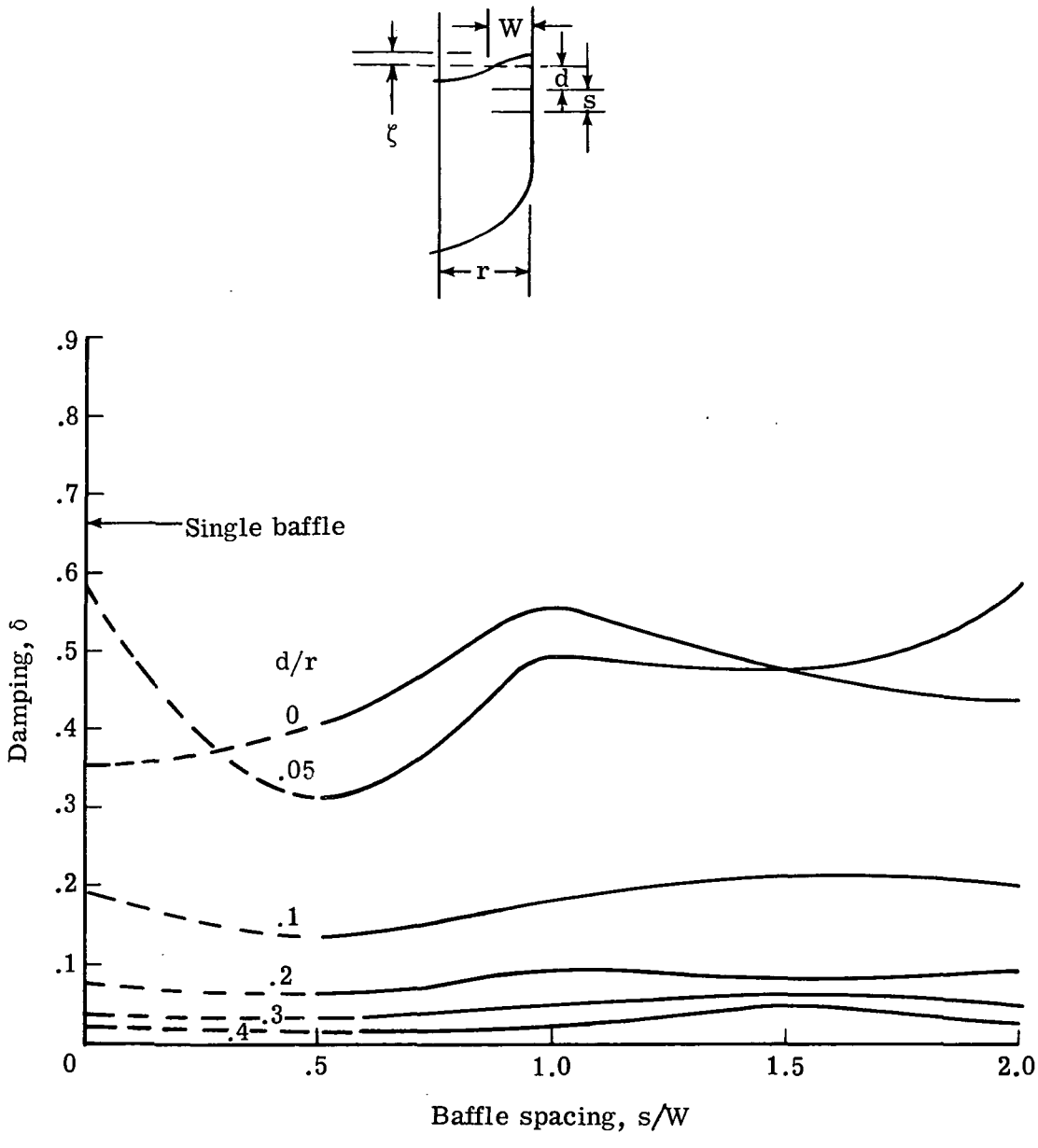

(a) $\zeta/R = 0.02$.

Figure 13.- Effect of multiple baffle spacing on liquid damping for a range of baffle depths.

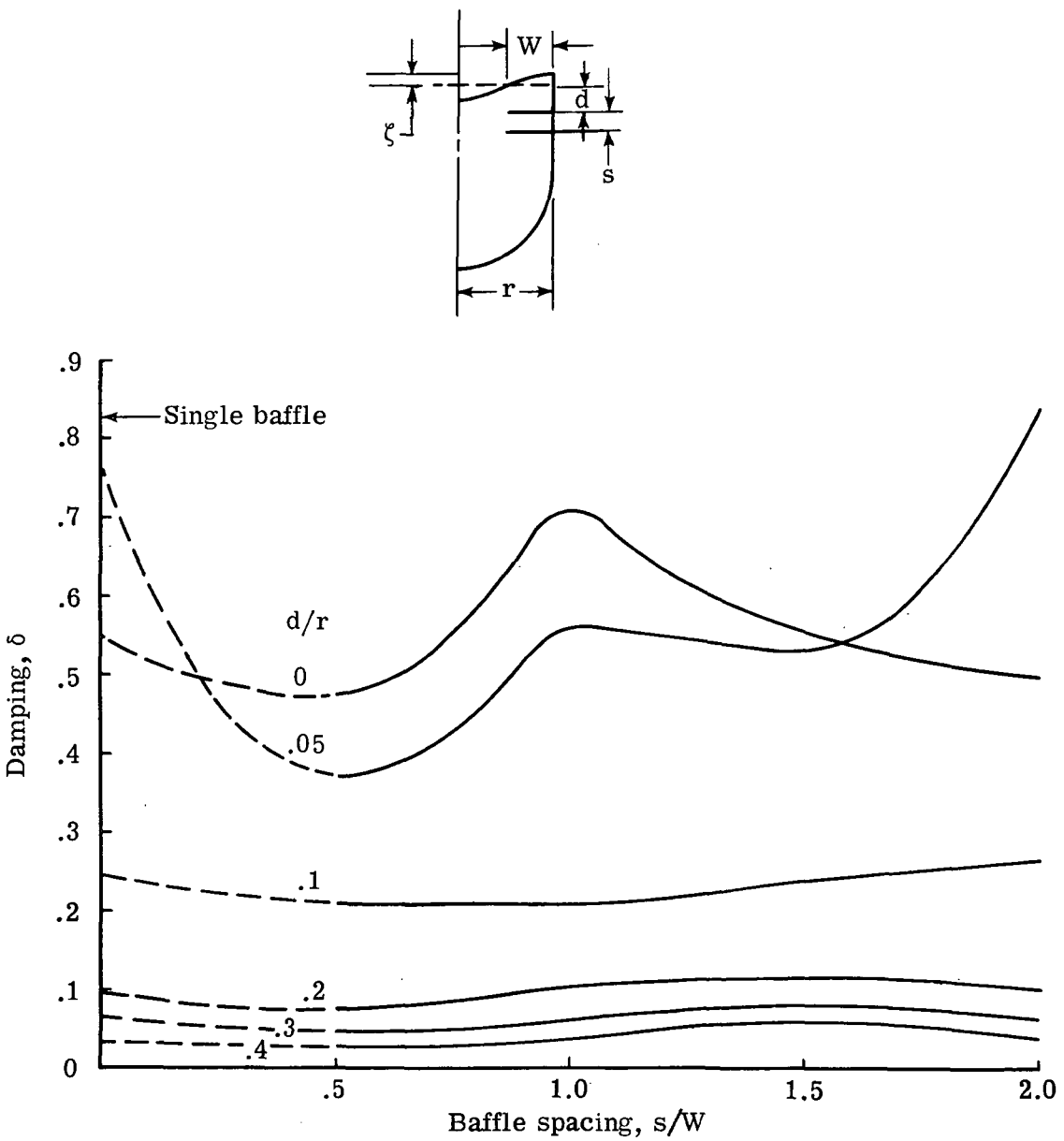

(b) $\zeta/R = 0.04$.

Figure 13.- Concluded.

NASA-Langley, 1972 —— 2 L-8352

NATIONAL AERONAUTICS AND SPACE ADMINISTRATION
WASHINGTON, D.C. 20546

OFFICIAL BUSINESS
PENALTY FOR PRIVATE USE $300

SPECIAL FOURTH-CLASS RATE BOOK

POSTAGE AND FEES PAID
NATIONAL AERONAUTICS AND SPACE ADMINISTRATION
451

U.S.MAIL

POSTMASTER : If Undeliverable (Section 158 Postal Manual) Do Not Return

"The aeronautical and space activities of the United States shall be conducted so as to contribute . . . to the expansion of human knowledge of phenomena in the atmosphere and space. The Administration shall provide for the widest practicable and appropriate dissemination of information concerning its activities and the results thereof."

—NATIONAL AERONAUTICS AND SPACE ACT OF 1958

NASA SCIENTIFIC AND TECHNICAL PUBLICATIONS

TECHNICAL REPORTS: Scientific and technical information considered important, complete, and a lasting contribution to existing knowledge.

TECHNICAL NOTES: Information less broad in scope but nevertheless of importance as a contribution to existing knowledge.

TECHNICAL MEMORANDUMS: Information receiving limited distribution because of preliminary data, security classification, or other reasons. Also includes conference proceedings with either limited or unlimited distribution.

CONTRACTOR REPORTS: Scientific and technical information generated under a NASA contract or grant and considered an important contribution to existing knowledge.

TECHNICAL TRANSLATIONS: Information published in a foreign language considered to merit NASA distribution in English.

SPECIAL PUBLICATIONS: Information derived from or of value to NASA activities. Publications include final reports of major projects, monographs, data compilations, handbooks, sourcebooks, and special bibliographies.

TECHNOLOGY UTILIZATION PUBLICATIONS: Information on technology used by NASA that may be of particular interest in commercial and other non-aerospace applications. Publications include Tech Briefs, Technology Utilization Reports and Technology Surveys.

Details on the availability of these publications may be obtained from:

SCIENTIFIC AND TECHNICAL INFORMATION OFFICE

NATIONAL AERONAUTICS AND SPACE ADMINISTRATION

Washington, D.C. 20546